

Expectation Propagation for Nonlinear Inverse Problems

– with an Application to Electrical Impedance Tomography

Matthias Gehre* Bangti Jin†

September 28, 2018

Abstract

In this paper, we study a fast approximate inference method based on expectation propagation for exploring the posterior probability distribution arising from the Bayesian formulation of nonlinear inverse problems. It is capable of efficiently delivering reliable estimates of the posterior mean and covariance, thereby providing an inverse solution together with quantified uncertainties. Some theoretical properties of the iterative algorithm are discussed, and the efficient implementation for an important class of problems of projection type is described. The method is illustrated with one typical nonlinear inverse problem, electrical impedance tomography with complete electrode model, under sparsity constraints. Numerical results for real experimental data are presented, and compared with that by Markov chain Monte Carlo. The results indicate that the method is accurate and computationally very efficient.

Keywords: expectation propagation, nonlinear inverse problem, uncertainty quantification, sparsity constraints, electrical impedance tomography

1 Introduction

In this work, we study a statistical method, Expectation Propagation (EP), for inferring the mean and covariance of posterior distributions arising in the Bayesian formulation of either linear or nonlinear inverse problems. The EP method was first developed in the machine learning community [38, 39], to efficiently arrive at an approximation. In contrast to popular Markov chain Monte Carlo (MCMC) methods [21, 35], the EP is far less expensive yet with little compromise in the accuracy [42].

*Center for Industrial Mathematics, University of Bremen, Bremen D-28344, Germany (mgehre@math.uni-bremen.de)

†Department of Mathematics, University of California, Riverside, University Ave. 900, Riverside, California 92521, USA (bangti.jin@gmail.com)

1.1 Bayesian formulation

We consider a (possibly nonlinear) equation

$$F(x) = b, \tag{1}$$

where the map $F : \mathbb{R}^n \rightarrow \mathbb{R}^m$, and vectors $x \in \mathbb{R}^n$ and $b \in \mathbb{R}^m$ refer to the data formation mechanism, the unknowns and the given data, respectively. In the context of inverse problems related to differential equations, the map F often involves a discretized solution operator of the underlying governing differential equation. In practice, we only have access to a noisy version b of the exact data b^\dagger , i.e., $b = b^\dagger + \zeta$, where the vector $\zeta \in \mathbb{R}^m$ represents the noise in the data.

The Bayesian approach has received increasing attention in recent years [32] due to its distinct features compared with conventional deterministic inversion techniques. In this work, we are interested in the fast exploration of the resulting Bayesian posterior distribution. We first briefly recall the fundamentals of the Bayesian approach. There are two basic building blocks of Bayesian modeling, i.e., the likelihood function and the prior distribution. The likelihood function $p(b|x)$ depends on the statistics of the noise ζ . The most popular choice in practice is the Gaussian model, i.e., ζ follows a normal distribution with mean zero and variance $\sigma^2 I_m$, or $p(\zeta) = (\sqrt{2\pi\sigma^2})^{-m} e^{-\frac{1}{2\sigma^2} \|\zeta\|_2^2}$, where $\|\cdot\|_r$, $r \geq 1$, refers to the r -norm of a vector. This gives a likelihood function $p(b|x) \propto e^{-\frac{1}{2\sigma^2} \|F(x)-b\|_2^2}$. The Gaussian model is often justified by appealing to the central limit theorem. Another popular choice is the Laplace distribution on the noise ζ , i.e., $p(\zeta) = (2\sigma)^{-m} e^{-\frac{1}{\sigma} \|\zeta\|_1}$, which gives a likelihood function $p(b|x) \propto e^{-\frac{1}{\sigma} \|F(x)-b\|_1}$. The Laplace model is especially suited to data with a significant amount of outliers [12].

In Bayesian modeling, we encode our prior knowledge about the unknown x in a prior distribution $p(x)$, which forms the second building block of Bayesian modeling. The main role of the prior $p(x)$ is to regularize the ill-posedness inherent to the model (1) so as to achieve a physically meaningful solution [17]. Hence the effect of the prior $p(x)$ is pronounced for ill-posed and under-determined problems; its influence will vanish for a well-posed, invertible F as the noise-level tends to zero. There are many possible choices of the prior distribution $p(x)$, depending on the desired qualitative features of the sought-for solution: globally smooth, sparse (with respect to a certain basis), blocky and monotone etc. Typically such prior knowledge is encoded by a Markov random field. One popular choice is the smoothness prior, i.e., $p(x) = N(x; \mu_0, C_0)$, with mean μ_0 and covariance C_0 .

By Bayes' formula, we obtain the posterior distribution

$$p(x|b) \propto p(b|x)p(x)$$

up to a constant factor depending only on the data b . The posterior distribution $p(x|b)$ holds the full

information about the probability of any vector x explaining the observational data b . A very popular and straightforward approach is to search for the maximizing element x of the posterior distribution $p(x|b)$, which leads to the celebrated Tikhonov regularization. However, it only yields information about one point estimate from an ensemble of many equally plausible explanations, the posterior distribution $p(x|b)$, and further, it completely ignores the uncertainties associated with a particular solution.

1.2 Bayesian computations

Alternatively, one can compute the (conditional) mean of the unknown x given the data b to obtain “averaged” information about the unknown x , which is representative of the posterior distribution $p(x|b)$. Further, one can infer the associated uncertainty information respectively credible intervals by calculating the (conditional) variance of the unknown x . Numerically, the computation of the mean μ^* and covariance C^* entails the following high-dimensional integrals

$$\mu^* = \int p(x|b)x dx \quad \text{and} \quad C^* = \int p(x|b)(x - \mu^*)(x - \mu^*)^t dx,$$

which are intractable by means of classical numerical quadrature rules, except for the case of very low-dimensional problems, e.g., $n = 1, 2$. Instead, one can either resort to sampling through Markov Chain Monte Carlo (MCMC) methods [21, 35], or (deterministic) approximate inference methods, e.g., variational approximations [3, 26].

The MCMC is currently the most versatile and popular method for exploring the posterior state. It constructs a Markov chain with the posterior distribution $p(x|b)$ as its stationary distribution, and draws samples from the posterior by running the Markov chain, from which the sample mean and sample variance can be readily computed. We illustrate the computational challenge on the classical Metropolis-Hastings algorithm [21], cf. Algorithm 1. The algorithm generates a set of N dependent samples, and we use the sample mean and sample covariance to approximate μ^* and C^* . In order to obtain accurate estimates, a fairly large number of samples (after discarding the initial samples) are required, e.g., $N = 1 \times 10^5 \sim 1 \times 10^6$. At each iteration of the algorithm, one needs to evaluate the acceptance probability $\rho(x^{(k)}, x^{(*)})$, in order to determine whether the proposal $x^{(*)}$ should be accepted. In turn, this essentially boils down to evaluating the likelihood $p(b|x^{(*)})$ (and the prior $p(x^{(*)})$, which is generally much cheaper), and thus invokes the forward simulation $F(x^{(*)})$. In the context of inverse problems for differential equations, it amounts to solving one partial differential equation (system) for the proposed parameter vector $x^{(*)}$. However, for many practical applications, e.g., underground flow, wave propagation, geophysics, chemical kinetics and nonlinear tomography, each forward simulation is already expensive, and thus a straightforward application of the Metropolis-Hastings algorithm is prohibitively expensive, if not impractical at all.

Algorithm 1 Metropolis-Hastings algorithm for sampling from $p(x|b)$

```
1: Set  $N$  and  $x^{(0)}$ , and select proposal distribution  $q(x|x')$ .
2: for  $k = 0 : N$  do
3:   draw sample  $x^{(*)}$  from  $q(x|x^{(k)})$ .
4:   compute the acceptance probability  $\rho(x^{(k)}, x^{(*)}) = \min\left(1, \frac{p(x^{(*)}|b)q(x^{(k)}|x^{(*)})}{p(x^{(k)}|b)q(x^{(*)}|x^{(k)})}\right)$ .
5:   generate  $u$  from uniform distribution  $U(0, 1)$ .
6:   if  $u \leq \rho(x^{(k)}, x^{(*)})$  then
7:      $x^{(k+1)} = x^{(*)}$ .
8:   else
9:      $x^{(k+1)} = x^{(k)}$ .
10:  end if
11: end for
```

Therefore, there have been many works on accelerating the Metropolis-Hastings algorithm. A first idea is to use surrogates for the expensive forward simulator, which directly reduces the cost of the sampling step. The surrogate can be constructed in many ways, including reduced-order modeling [25] and polynomial chaos [37] etc. The key is to construct faithful surrogates, which is typically viable only in low-dimensional parameter spaces. The second idea is to design problem-dependent proposal distributions. In practice, simple proposal distributions are not adapted to the specific problem structure, which is essentially true in case of inverse problems, where the Hessian of the forward map is generally highly smoothing (with a large-dimensional numerical kernel). Accordingly, the proposals are not well matched with the posteriori, and thus only few samples can be accepted and a large part of the expensive computations (used in forward simulation) is wasted. To this end, two effective strategies have been developed: One strategy relies on the idea of preconditioning, which screens the proposal with inexpensive preconditioner, typically low-resolution forward simulators or cheap surrogates [24, 14, 11]. The other strategy gleans optimization theory and exploits the Hessian of the forward map for effective sample generation, e.g., Langevin methods [46] and Hessian information [23, 16, 36].

Despite these impressive progresses, the application of these approaches to complex Bayesian models, such as those arising in inverse problems for differential equations, remains challenging and highly non-trivial, and there has been considerable interest in developing fast alternatives. Approximate inference methods, e.g., variational methods [30, 3] and expectation propagation [38, 39], belong to this group. Approximate inference methods often approximate the posterior distribution with computationally more trackable distributions, in the hope of capturing the specific structure of the problem, and typically involve a sequence of optimization/integration problems. The accuracy of these approximate methods depends crucially on the adopted simplifying assumptions, but generally cannot be made arbitrarily accurate. This is in stark contrast to the MCMC, which in theory can be made arbitrarily accurate by running the Markov chain long enough. Nonetheless, often they can offer a reasonable approximation within a small fractional of computing time needed for the MCMC, and therefore have received increasing attention

in practical applications. Recently, a different optimization approach based on the idea of transporting the prior into the posterior via polynomial maps was developed in [15], where the degree of polynomial restricts the accuracy of the approximation.

In this work, we study the EP method [38, 39] for numerically exploring the posterior distribution. The EP method is of deterministic optimization nature. Algorithmically, it iteratively adjusts the iterates within the Gaussian family by minimizing the Kullback-Leibler divergence and looping over all the factors in likelihood/prior in a manner analogous to the classical Kaczmarz method [31] for solving a linear system of equations. The EP generally delivers an approximation with reasonable accuracy [42].

1.3 Our contributions

The goal of the present work is to study the EP method, and to demonstrate its significant potentials for (nonlinear) inverse problems. We shall discuss the basic idea, theoretical properties, and the efficient implementation for an important class of Bayesian formulations.

Our main contributions are as follows. Theoretically, we discuss well-definedness of the EP method in the multi-dimensional case (Theorem 2.2), which extends a known result [44]. We provide additional theoretical insight into the algorithm for some problems with special structures. Algorithmically, we propose a coupling of the EP method with an iterative linearization strategy to handle nonlinear inverse problems. Further, numerical results for one representative nonlinear inverse problem, electrical impedance tomography (EIT) with real experimental data on a water tank, under sparsity constraints, will be presented. To the best of our knowledge, this represents the first application of the EP method to a PDE-constrained inverse problem.

The sparsity approach for EIT has recently been revisited in [19] in the framework of classical regularization, and this work extends the deterministic model to a Bayesian setting. The extension provides valuable insights into the sparsity imaging technique, e.g., the reliability of a particular solution. The numerical results indicate that with proper implementation, the EP method can deliver approximations with good accuracy to the posterior mean and covariance for EIT imaging, within a small fraction of computational efforts required for the MCMC.

The rest of the paper is organized as follows. In Section 2, we describe the basic idea of the EP algorithm, and discuss some theoretical properties. In Sections 3 and 4, we discuss the efficient implementation of a special class of problems, and present numerical results for EIT imaging to illustrate its accuracy and efficiency. In the appendices, we collect some auxiliary results and technical proofs.

2 EP Theory

In this part, we describe the expectation propagation (EP) algorithm for approximate Bayesian inference of a generic probability distribution that can be factorized into a specific form. We begin with the basic idea and algorithm, and then discuss some properties.

2.1 Basic idea

The goal of the EP algorithm is to construct a Gaussian approximation to a generic distribution $p(x)$. It [38, 39] approximates the distribution $p(x)$ by a Gaussian distribution $\tilde{p}(x)$. To this end, we first factorize the target distribution $p(x)$ into

$$p(x) = \prod_{i \in I} t_i(x).$$

where I is a finite index set for the factors, which is often omitted below for notational simplicity. The optimal factorization is dependent on the specific application. Then a Gaussian approximation $\tilde{t}_i(x)$ to each factor $t_i(x)$ is sought after by minimizing the difference between the following two distributions

$$\prod_j \tilde{t}_j(x) \quad \text{and} \quad t_i(x) \prod_{j \neq i} \tilde{t}_j(x)$$

for every i . Following [38], we measure the difference between two probability distributions p and q by the Kullback-Leiber divergence $D_{KL}(p, q)$ (also known as relative entropy and information gain etc. in the literature) [34] defined by

$$D_{KL}(p, q) = \int p(x) \log \frac{p(x)}{q(x)} dx.$$

In view of Jensen's inequality, the Kullback-Leibler divergence $D_{KL}(p, q)$ is always nonnegative, and it vanishes if and only if $p = q$ almost everywhere. However it is not symmetric and does not satisfy the triangle inequality, and thus it is not a metric.

Nonetheless, the divergence $D_{KL}(p, q)$ has been very popular in measuring of the difference between two probability distributions p and q . Specifically, the divergence of q from p , denoted $D_{KL}(p, q)$, is a measure of the information lost when q is used to approximate p , which underlies the EP algorithm and many other approximations, e.g., variational method [3, 30] and coarse graining [9, 4].

Specifically, we update the factor approximation $\tilde{t}_i(x)$ by

$$\tilde{t}_i(x) = \arg \min_{\tilde{q} \text{ Gaussian}} D_{KL} \left(t_i(x) \prod_{j \neq i} \tilde{t}_j(x), \tilde{q}(x) \prod_{j \neq i} \tilde{t}_j(x) \right). \quad (2)$$

Intuitively, the goal of the update $\tilde{t}_i(x)$ is to “learn” the information contained in the factor $t_i(x)$, and

by looping over all factors, hopefully the essential characteristics of the posterior $p(x)$ are captured. We observe that even though each update involves only a “local” problem, the influence is global due to the presence of the term $\prod_{j \neq i} \tilde{t}_j(x)$.

2.2 Minimizing D_{KL} and basic algorithm

The central task in the EP algorithm is to compute the minimizers to the Kullback-Leibler divergences, i.e., Gaussian factors $\tilde{t}_j(x)$. To this end, we first consider the general problem of minimizing the Kullback-Leibler divergence $D_{KL}(q, \tilde{q})$ between a non-gaussian distribution $q(x)$ and a Gaussian distribution $\tilde{q}(x) = N(x; \mu, C)$ with respect to \tilde{q} , which is shown in the next result. We note that the minimizer \tilde{q} is completely determined by the mean μ and covariance C .

Theorem 2.1. *Let q be a probability distribution with a finite second moment, $\mu^* = E_q[x]$ and $C^* = \text{Var}_q[x]$. Then there exists a minimizer to*

$$\min_{\tilde{q} \text{ Gaussian}} D_{KL}(q, \tilde{q})$$

over any compact set of Gaussians with a positive definite covariance. Further, if $N(x; \mu^, C^*)$ belongs to the interior of the compact set, then it is a local minimizer.*

Proof. The existence follows directly from the compactness assumption, and the continuity of Kullback-Leibler divergence in the second argument. Let $\tilde{q}(x) = N(x; \mu, C)$. The divergence $D_{KL}(q, \tilde{q})$ can be expanded into

$$D_{KL}(q, \tilde{q}) = \int q(x) \left(\log q(x) + \frac{d}{2} \log 2\pi - \frac{1}{2} \log |C^{-1}| + \frac{1}{2} (\mu - x)^t C^{-1} (\mu - x) \right) dx.$$

We first compute the gradient $\nabla_{\mu} D_{KL}(q, \tilde{q})$ of the divergence $D_{KL}(q, \tilde{q})$ with respect to the mean μ of the Gaussian factor $\tilde{q}(x)$, i.e.,

$$\nabla_{\mu} D_{KL}(q, \tilde{q}) = \int q(x) C^{-1} (\mu - x) dx,$$

and set it to zero to obtain the first condition $\mu = E_q[x]$.

Likewise, we compute the gradient $\nabla_P D_{KL}(q, \tilde{q})$ of $D_{KL}(q, \tilde{q})$ with respect to the precision $P = C^{-1}$

$$\nabla_P D_{KL}(q, \tilde{q}) = \int q(x) \left(-\frac{1}{2} P^{-1} + \frac{1}{2} (\mu - x)(\mu - x)^t \right) dx,$$

where we have used the following matrix identities [13]

$$\frac{\partial}{\partial A} \log |A| = A^{-1}, \quad x^t A x = \text{tr}(A x x^t) \quad \text{and} \quad \frac{\partial}{\partial A} \text{tr}(AB) = B^t.$$

The gradient $\nabla_P D_{KL}(q, \tilde{q})$ vanishes if and only if the condition $C = E_q[(x - \mu)(x - \mu)^t]$ holds. Together with the condition on the mean μ , this is equivalent to $C = \text{Var}_q[x]$. Now the second assertion follows from the convexity of the divergence in the second argument and the assumption that $N(x; \mu^*, C^*)$ is an interior point of the compact set. \square

The method is called Expectation Propagation (EP) because it propagates the expectations of x and $x x^t$ under the true distribution p to the Gaussian approximation \tilde{p} . By Theorem 2.1, minimizing $D_{KL}(q, \tilde{q})$ involves computing (possibly very high-dimensional) integrals. It is feasible only if the integrals can be reduced to a low-dimensional case. One such case will be discussed in Section 3. Now we can state the basic EP algorithm; see Algorithm 2. The stopping criterion at Step 7 can be based on monitoring the relative changes of the approximate Gaussian factors $\tilde{t}_i(x)$.

Algorithm 2 Approximate the posterior $p(x) = \prod_i t_i(x)$ by $\prod_i \tilde{t}_i(x)$ with Gaussian factors $\{\tilde{t}_i\}$.

- 1: Start with initial distributions $\{\tilde{t}_i\}$
 - 2: **while** not converged **do**
 - 3: **for** $i \in I$ **do**
 - 4: Calculate $\tilde{q}(x)$ to $t_i(x) \prod_{j \neq i} \tilde{t}_j(x)$ by $\min_{\text{Gaussian } \tilde{q}} D_{KL}(t_i(x) \prod_{j \neq i} \tilde{t}_j(x), \tilde{q}(x))$
 - 5: Set $\tilde{t}_i(x) = \frac{\tilde{q}(x)}{\prod_{j \neq i} \tilde{t}_j(x)}$
 - 6: **end for**
 - 7: Check the stopping criterion.
 - 8: **end while**
-

Remark 2.1. *The EP method estimates both the mean and covariance of the posterior distribution. In some cases, the mean might be close to the maximum a posteriori estimate. Since the latter can be efficiently computed via modern minimization algorithms, then the EP algorithm should be adapted to estimate the covariance only. We shall not delve into the adaptation here, and leave it to a future work.*

2.3 Basic properties of EP algorithm

In general, the convergence of the EP algorithm remains fairly unclear, and nonconvergence has been observed for a naive implementation of the algorithm, especially for the case that the factors are not log-concave, like the t likelihood/prior. In this part, we collect some results on the convergence issue.

Our first result is concerned with the exact recovery for Gaussian factors within one step.

Proposition 2.1. *Let the factors $\{t_i\}$ be Gaussian. Then the EP algorithm converges after updating each factor approximation once with the limit $\tilde{t}_i = t_i$, $i \in I$.*

Proof. By the definition of the EP algorithm, the i th factor \tilde{t}_i is found by $\arg \min_{\tilde{q}} D_{\text{KL}}^{\text{Gaussian}} \left(t_i \prod_{j \neq i} \tilde{t}_j, \tilde{q} \right)$. Due to the Gaussian assumption on the factor t_i , the choice $\tilde{q} = t_i \prod_{j \neq i} \tilde{t}_j$ is Gaussian and it minimizes the Kullback-Leibler divergence with a minimum value zero, i.e., $\tilde{t}_i = t_i$. Clearly one sweep exactly recovers all the factors. \square

The next result shows the one-step convergence for the case of decoupled factors, i.e., $t_j(x) = t_j(x_j)$ with the partition $\{x_j\}$ of x being pairwise disjoint. It is an analogue to the Gauss-Seidel iteration method for a linear system of equations with a diagonal matrix. We will provide a constructive proof, which relies on Theorem 3.1 below, and hence it is deferred to Appendix A.

Proposition 2.2. *Let $q(x) = \prod t_i(x_i)$, and $\{x_i\}$ form a pairwise disjoint partition of the vector $x \in \mathbb{R}^n$. If the factors $\tilde{t}_i(x)$ are initialized as $\tilde{t}_i(x) = \tilde{t}_i(x_i)$ then the EP algorithm converges after one iteration and the limit iterate $\{\tilde{t}_i\}$ satisfies the moment matching conditions.*

A slightly more general case than Proposition 2.2 is the case of a linear system with a “triangular-shaped” matrix. Then one naturally would conjecture that the convergence is reached within a finite number of iterations. However, it is still unclear whether this is indeed the case.

The next result shows the well-definedness of the EP algorithm for log-concave factors. The proof requires several technical lemmas in Appendix B. The result is essentially a restatement of [44, Theorem 1]. We note that the proof in [44] is for the one-dimensional case, whereas the proof below is multi-dimensional. Further, we specify more clearly the conditions.

Theorem 2.2. *Let the factors $\{t_i\}$ in the posterior $\prod t_i(x)$ be log-concave, uniformly bounded and have support of positive measure. If at iteration k , the factor covariances $\{C_i\}$ of the approximations $\{\tilde{t}_i\}$ are positive definite, then the EP updates at $k + 1$ step are positive semidefinite.*

Proof. By the positive definiteness of the factor covariances $\{C_i\}$, the covariance $C_{\setminus i}$ of the cavity distribution $\tilde{t}_{\setminus i} = \prod_{j \neq i} \tilde{t}_j$ is positive definite. Next we show that the partition function $Z = \int N(x; \mu_{\setminus i}, C_{\setminus i}) t_i(x) dx$ is log-concave in $\mu_{\setminus i}$. A straightforward computation yields that $N(x; \mu_{\setminus i}, C_{\setminus i})$ is log-concave in $(x, \mu_{\setminus i})$. By Lemma B.3 and log-concavity of $t_i(x)$, $N(x; \mu_{\setminus i}, C_{\setminus i}) t_i(x)$ is log-concave in $(x, \mu_{\setminus i})$, and thus Lemma B.4 implies that Z is log-concave in $\mu_{\setminus i}$, and $\nabla_{\mu_{\setminus i}}^2 \log Z$ is negative semi-definite.

Now by Lemma B.1, the covariance C of $Z^{-1} N(x; \mu_{\setminus i}, C_{\setminus i}) t_i(x)$ is given by

$$C = C_{\setminus i} \left(\nabla_{\mu_{\setminus i}}^2 \log Z \right) C_{\setminus i} + C_{\setminus i}.$$

Meanwhile, by the boundedness of factors t_i , the covariance $Z^{-1} \int N(x; \mu_{\setminus i}, C_{\setminus i}) t_i(x) (x - \mu^*) (x - \mu^*)^t dx$ (with $\mu^* = Z^{-1} \int N(x; \mu_{\setminus i}, C_{\setminus i}) t_i(x) x dx$) exists, and further by Lemma B.2 and the assumption on t_i , it is positive definite. Hence, C is positive definite.

Since the Hessian $\nabla_{\mu_{\setminus i}}^2 \log Z$ is negative semi-definite, $C - C_{\setminus i} = C_{\setminus i} \left(\nabla_{\mu_{\setminus i}}^2 \log Z \right) C_{\setminus i}$ is also negative semi-definite, i.e., for any vector w , $w^t C w \leq w^t C_{\setminus i} w$. Now we let $\tilde{w} = C^{\frac{1}{2}} w$. Then $\|\tilde{w}\|^2 \leq \tilde{w}^t C^{-\frac{1}{2}} C_{\setminus i} C^{-\frac{1}{2}} \tilde{w}$ for any vector \tilde{w} . By the minmax characterization of eigenvalues of a Hermitian matrix, $\lambda_{\min}(C^{-\frac{1}{2}} C_{\setminus i} C^{-\frac{1}{2}}) \geq 1$. Consequently, $\lambda_{\max}(C^{\frac{1}{2}} C_{\setminus i}^{-1} C^{\frac{1}{2}}) \leq 1$, and equivalently $\|\tilde{w}\|^2 \geq \tilde{w}^t C^{\frac{1}{2}} C_{\setminus i}^{-1} C^{\frac{1}{2}} \tilde{w}$ for any vector \tilde{w} . With the substitution $w = C^{\frac{1}{2}} \tilde{w}$, we get $w^t C^{-1} w \geq w^t C_{\setminus i}^{-1} w$ for any vector w , i.e., $C^{-1} - C_{\setminus i}^{-1}$ is positive semidefinite. The conclusion follows from this and the fact that the inverse covariance of the factor approximation \tilde{t}_i is given by $C^{-1} - C_{\setminus i}^{-1}$. \square

Remark 2.2. *Theorem 2.2 only ensures the well-definedness of the EP algorithm for one iteration. One might expect that in case of strictly log-concave factors, the well-definedness holds for all iterations. However, this would require a strengthened version of the Prékopa-Leindler inequality, i.g., preservation of strict log-concavity under marginalization.*

3 EP with projections

Now we develop an applicable EP scheme by assuming that, apart from the Gaussian base $t_0(x)$, each factor involves a probability density function of the form $t_i(U_i x)$, i.e.,

$$t_0(x) \prod_i t_i(U_i x), \quad (3)$$

where the matrices U_i have full rank, and can represent either the projection onto several variables or linear combinations of the variables. The specific form of U_i depends on concrete applications. It occurs e.g., in robust formulation with the Laplace likelihood [18] and total variation prior. It represents an important structural property, and should be utilized to design efficient algorithms. The goal of this part is to derive necessary modifications of the basic EP algorithm and to spell out all the implementation details, following the very interesting works [47].

Each factor $t_i(U_i x)$ effectively depends on x through $U_i x$, albeit it lives on a high-dimensional space (that of x). This enables us to derive concise formulas for the mean and the covariance under the product density of one nongaussian factor $t_i(U_i x)$ and a Gaussian; see the following result. The proof follows from a standard but tedious change of variable, and hence it is deferred to Appendix C.

Theorem 3.1. *Let $\mu \in \mathbb{R}^n$, $C \in \mathbb{R}^{n \times n}$ be symmetric positive definite and $U \in \mathbb{R}^{l \times n}$ ($l \leq n$) be of full rank, $Z = \int t(Ux) N(x; \mu, C) dx$ be the normalizing constant. Then the mean $\mu^* = E_{Z^{-1} t(Ux) N(x; \mu, C)}[x]$*

and covariance $C^* = \text{Var}_{Z^{-1}t(Ux)N(x;\mu,C)}[x]$ are given by

$$\begin{aligned}\mu^* &= \mu + CU^t(UCU^t)^{-1}(\bar{s} - U\mu), \\ C^* &= C + CU^t(UCU^t)^{-1}(\bar{C} - UCU^t)(UCU^t)^{-1}UC,\end{aligned}$$

where $\bar{s} \in \mathbb{R}^l$ and $\bar{C} \in \mathbb{R}^{l \times l}$ are respectively given by

$$\bar{s} = E_{Z^{-1}t(s)N(s;U\mu,UCU^t)}[s] \quad \text{and} \quad \bar{C} = \text{Var}_{Z^{-1}t(s)N(s;U\mu,UCU^t)}[s].$$

Now we can present the EP algorithm for the approximate inference of the posterior distribution (3); see Algorithm 3. We shall skip the update of the Gaussian factor $t_0(x)$. Here we have adopted the following canonical representation of the Gaussian approximation $\tilde{t}_i(U_i x)$ to $t_i(U_i x)$, i.e.,

$$\tilde{t}_i(U_i x) \propto \exp\left((U_i x)^t h_i - \frac{1}{2}(U_i x)^t K_i (U_i x)\right), \quad (4)$$

where h_i and K_i are low-rank parameters to be updated. With the representation (4), there holds

$$\begin{aligned}\tilde{t}_i(x) &= N(x; \mu_i, C_i) \propto e^{-\frac{1}{2}(x-\mu_i)^t C_i^{-1}(x-\mu_i)} \\ &\propto e^{-\frac{1}{2}x^t C_i^{-1}x + x^t C_i^{-1}\mu_i} =: G(x, h_i, K_i),\end{aligned}$$

with $h_i = C_i^{-1}\mu_i$ and $K_i = C_i^{-1}$. Then the approximate distribution $\prod_i \tilde{t}_i(U_i x)$ is a Gaussian distribution with parameters

$$K = K_0 + \sum_i U_i^t K_i U_i \quad \text{and} \quad h = h_0 + \sum_i U_i^t h_i,$$

where (K_0, h_0) is the parameter tuple of the Gaussian base t_0 .

The inner loop in Algorithm 3 spells out the minimization step in Algorithm 2 using the representation (4) and Theorem 3.1. In brevity, Steps 6–7 form the (cavity) distribution $\tilde{p}^{\setminus i} = t_0 \prod_{j \neq i} \tilde{t}_j(U_j x)$, i.e., mean $\mu_{\setminus i}$ and covariance $C_{\setminus i}$, and the low-rank representation $\hat{C}_i = U_i C_{\setminus i} U_i^t$ and $\hat{\mu}_i = U_i \mu_{\setminus i}$; Steps 8–9 update the parameters pair (h_i, K_i) for the i th gaussian factor $\tilde{t}_i(U_i x)$. Steps 10–11 then update the global approximation (h, K) by the new values for the i th factor. There is a parallel variant of the EP algorithm, where steps 10–11 are moved behind the inner loop. The parallel version can be much faster on modern multi-core architectures, since it scales linearly in the number of processors, but it is less robust than the serial variant. Now we derive the main steps of Algorithm 3.

(i) Step 6 forms the covariance of the cavity distribution $\tilde{p}^{\setminus i}$: From the elementary relation

$$G(x, h, K)/G(x, U_i^t h_i, U_i^t K_i U_i) = G(x, h - U_i^t h_i, K - U_i^t K_i U_i), \quad (5)$$

Algorithm 3 Serial EP algorithm with projection.

- 1: Initialize with $K_0 = C_0^{-1}$, $h_0 = C_0^{-1}\mu_0$, $K_i = I$ and $h_i = 0$ for $i \in I$
 - 2: $K = K_0 + \sum_i U_i^t K_i U_i$
 - 3: $h = h_0 + \sum_i U_i^t h_i$
 - 4: **while** not converged **do**
 - 5: **for** $i \in I$ **do**
 - 6: $\widehat{C}_i^{-1} = (U_i K^{-1} U_i^t)^{-1} - K_i$
 - 7: $\widehat{\mu}_i = (I - U_i K^{-1} U_i^t K_i)^{-1} (U_i K^{-1} h - U_i K^{-1} U_i^t h_i)$
 - 8: $K_i = \text{Var}_{Z^{-1}t_i(s_i)N(s_i; \widehat{\mu}_i, \widehat{C}_i)}[s_i]^{-1} - \widehat{C}_i^{-1}$, with $Z = \int t_i(s_i)N(s_i; \widehat{\mu}_i, \widehat{C}_i) ds_i$
 - 9: $h_i = \text{Var}_{Z^{-1}t_i(s_i)N(s_i; \widehat{\mu}_i, \widehat{C}_i)}[s_i]^{-1} E_{Z^{-1}t_i(s_i)N(s_i; \widehat{\mu}_i, \widehat{C}_i)}[s_i] - \widehat{C}_i^{-1} \widehat{\mu}_i$
 - 10: $K = K_0 + \sum_i U_i^t K_i U_i$
 - 11: $h = h_0 + \sum_i U_i^t h_i$
 - 12: **end for**
 - 13: Check the stopping criterion.
 - 14: **end while**
 - 15: Output the covariance $C = K^{-1}$ and the mean $\mu = K^{-1}h$.
-

we directly get the cavity covariance $C_{\setminus i} = (K - U_i^t K_i U_i)^{-1}$. Consequently, by Woodbury's formula [52]

$$(A + WCV)^{-1} = A^{-1} - A^{-1}W(C^{-1} + VA^{-1}W)^{-1}VA^{-1}, \quad (6)$$

and letting $\widehat{K}_i = U_i K^{-1} U_i^t$, we arrive at a direct formula for computing

$$\begin{aligned} \widehat{C}_i &= U_i^t C_{\setminus i} U_i = U_i^t (K - U_i^t K_i U_i)^{-1} U_i^t \\ &= U_i \left[K^{-1} - K^{-1} U_i^t (-K_i^{-1} + \widehat{K}_i)^{-1} U_i K^{-1} \right] U_i^t \\ &= \left[I + \widehat{K}_i K_i (I - \widehat{K}_i K_i)^{-1} \right] \widehat{K}_i = (I - \widehat{K}_i K_i)^{-1} \widehat{K}_i. \end{aligned}$$

Now inverting the matrix gives the cavity covariance $\widehat{C}_i^{-1} = \widehat{K}_i^{-1} - K_i$.

- (ii) Step 7 forms the cavity mean $\widehat{\mu}_i = U_i \mu_{\setminus i}$. In view of the identity (5), we have $\mu_{\setminus i} = (K - U_i^t K_i U_i)^{-1} (h - U_i^t h_i)$, and consequently

$$\begin{aligned} \widehat{\mu}_i &= U_i (K - U_i^t K_i U_i)^{-1} (h - U_i^t h_i) \\ &= U_i \left[K^{-1} - K^{-1} U_i^t (-K_i^{-1} + \widehat{K}_i)^{-1} U_i K^{-1} \right] (h - U_i^t h_i) \\ &= \left[I - \widehat{K}_i (-K_i^{-1} + \widehat{K}_i)^{-1} \right] (U_i K^{-1} h - \widehat{K}_i h_i) \\ &= \left[I + \widehat{K}_i K_i (I - \widehat{K}_i K_i)^{-1} \right] (U_i K^{-1} h - \widehat{K}_i h_i) \\ &= (I - \widehat{K}_i K_i)^{-1} (U_i K^{-1} h - \widehat{K}_i h_i). \end{aligned}$$

- (iii) Steps 8 and 9 updates the parameter (K_i, h_i) of the Gaussian approximation $\tilde{t}_i(U_i x)$. It relies on

the Gaussian approximation $p^*(x) = N(x; \mu^*, C^*)$ to $t_i(U_i x) \hat{p}^{\setminus i}(x)$, i.e.,

$$\tilde{t}_i(U_i x) \propto p^*(x) / \hat{p}^{\setminus i}(x).$$

Thus one first needs to derive the mean μ^* and the covariance C^* in Theorem 2.1. By Theorem 3.1, with $Z = \int t_i(s_i) N(s_i, \hat{\mu}_i, \hat{C}_i) ds_i$ and

$$\bar{p}_i(s_i) = Z^{-1} t_i(s_i) N(s_i, \hat{\mu}_i, \hat{C}_i),$$

we have

$$\begin{aligned} \mu^* &= \mu_{\setminus i} + C_{\setminus i} U_i^t \hat{C}_i^{-1} (E_{\bar{p}_i}[s_i] - U_i \mu_{\setminus i}), \\ C^* &= C_{\setminus i} + C_{\setminus i} U_i^t \hat{C}_i^{-1} (\text{Var}_{\bar{p}_i}[s_i] - \hat{C}_i) \hat{C}_i^{-1} U_i C_{\setminus i}. \end{aligned} \quad (7)$$

Therefore, the Gaussian factor \tilde{t}_i , i.e., (h_i, K_i) , is determined by $C^{*-1} - C_{\setminus i}^{-1}$ and $(C^*)^{-1} \mu^* - (C_{\setminus i})^{-1} \mu_{\setminus i}$, respectively. To this end, we first let

$$C = (\text{Var}_{\bar{p}_i}[s_i] - \hat{C}_i)^{-1} + \hat{C}_i^{-1} U_i C_{\setminus i} (C_{\setminus i})^{-1} C_{\setminus i} U_i^t \hat{C}_i^{-1} = (\text{Var}_{\bar{p}_i}[s_i] - \hat{C}_i)^{-1} + \hat{C}_i^{-1},$$

where we have used the definition $\hat{C}_i = U_i C_{\setminus i} U_i^t$. Then it follows from (7) and Woodbury's formula (6) that

$$\begin{aligned} (C^*)^{-1} - (C_{\setminus i})^{-1} &= \left(C_{\setminus i} + C_{\setminus i} U_i^t \hat{C}_i^{-1} (\text{Var}_{\bar{p}_i}[s_i] - \hat{C}_i) \hat{C}_i^{-1} U_i C_{\setminus i} \right)^{-1} - (C_{\setminus i})^{-1} \\ &= - (C_{\setminus i})^{-1} C_{\setminus i} U_i^t \hat{C}_i^{-1} C^{-1} \hat{C}_i^{-1} U_i C_{\setminus i} (C_{\setminus i})^{-1} \\ &= - U_i^t \hat{C}_i^{-1} [(\text{Var}_{\bar{p}_i}[s_i] - \hat{C}_i)^{-1} + \hat{C}_i^{-1}]^{-1} \hat{C}_i^{-1} U_i \\ &= U_i^t (\text{Var}_{\bar{p}_i}[s_i]^{-1} - \hat{C}_i^{-1}) U_i. \end{aligned}$$

Analogously, we deduce from (7) and the above formula that

$$(C^*)^{-1} \mu^* - (C_{\setminus i})^{-1} \mu_{\setminus i} = U_i^t (\text{Var}_{\bar{p}_i}[s_i]^{-1} E_{\bar{p}_i}[s_i] - (\hat{C}_i)^{-1} U_i \mu_{\setminus i}).$$

By comparing these identities with the representation (4) for $\tilde{t}(U_i x)$, we arrived at the desired updating formulae in Steps 8–9 for the tuple (K_i, h_i) :

$$\begin{aligned} K_i &= \text{Var}_{\bar{p}_i}[s_i]^{-1} - \hat{C}_i^{-1}, \\ h_i &= \text{Var}_{\bar{p}_i}[s_i]^{-1} E_{\bar{p}_i}[s_i] - (\hat{C}_i)^{-1} U_i \mu_{\setminus i}. \end{aligned}$$

(iv) Steps 10–11 update the parameters (K, h) of the global approximation with the current parameters

of the i th factor. The update of K is implemented as a Cholesky up/downdate to the Cholesky factor of K . For example, computing the Cholesky factor \widehat{L} of the rank-one update $A \pm xx^t$ from the Cholesky factor L of $LL^t = A$ by Cholesky up/downdate is much faster than computing the Cholesky factor \widehat{L} directly [22]. In particular, for one-dimensional projection space, we use a Cholesky update with $x = U_i^t \sqrt{K_i}$ if $K_i > 0$ and a Cholesky downdate with $x = U_i^t \sqrt{-K_i}$ if $K_i < 0$. A Cholesky downdate may fail if the resulting matrix is no longer positive definite; see Theorem 2.2 for conditions ensuring positive definiteness.

The major computational efforts in the inner loop lie in computing the mean $\widehat{\mu}_i$ and the inverse covariance \widehat{C}_i^{-1} . The mean $E_{\widehat{p}_i}[s_i]$ and covariance $\text{Var}_{\widehat{p}_i}[s_i]$ necessitate integral, which is tractable if and only if the projections $\{U_i\}$ have very low-dimensional ranges. Our numerical examples with sparsity constraints in Section 4 involve only one-dimensional integrals.

Algorithm 3 is computable in exact arithmetic as long as the inverses can be computed. This hinges on the positive definiteness of K and $(U_i K^{-1} U_i^t)^{-1} - K_i$. Note that $\text{Var}_{\widehat{p}_i}[s_i]$ is positive definite by Lemma B.2 if the factors are nondegenerate. However, numerical instabilities can occur if those expressions become too close to singular. Choosing initial values for K_i gives some control over the condition of $K = K_0 + \sum_i U_i^t K_i U_i$ in the first iteration. However, general bounds for the conditioning of K at later iterations are still unknown.

Algorithm 4 EP for nonlinear problem $F(x) = b$.

- 1: Initialize with $\mu = \mu^0$
 - 2: **for** $k = 0 : \text{MaxIter}$ **do**
 - 3: Linearize around μ^k such that $F(x) \approx F(\mu^k) + F'(\mu^k)(x - \mu^k) + O(\|x - \mu^k\|_2^2)$
 - 4: Use Algorithm 3 to approximate the linearized problem with a Gaussian $N(\mu_*^k, C_*^k)$
 - 5: Compute Barzilai-Borwein step size τ^k
 - 6: Update $\mu^{k+1} = \mu^k + \tau^k(\mu_*^k - \mu^k)$
 - 7: Check the stopping criterion.
 - 8: **end for**
 - 9: Output the covariance C^* and the mean μ^* .
-

Now we discuss the case of a nonlinear operator F . To this end, we employ the idea of recursive linearization. The complete procedure is given in Algorithm 4, where MaxIter is the maximum number of iterations. Like most optimization algorithms based on linearization, step size control is often necessary. Only for problems with low degree of nonlinearity, the step size selection can be dropped by setting $\mu^{k+1} = \mu_*^k$, i.e., a step size of 1. Generally, it improves the robustness of the algorithm and avoids jumping back and forth between two states. There are many possible rules, and we only mention the Barzilai-Borwein rule here. It was proposed for gradient type methods in [2]. It approximates the Hessian by a scalar multiple of the identity matrix based on the last two iterates and descent directions so as to exploit the curvature information to accelerate/stabilize the descent into the minimum. Here we adopt

the following simple update rule

$$\mu^{k+1} = \mu^k + \tau^k(\mu_*^k - \mu^k),$$

and thus $\mu_*^k - \mu^k$ serves as a “descent” direction and μ^k acts as the iterate in the Barzilai-Borwein rule.

The step size τ^k is computed by

$$\tau^k = \frac{\langle \mu^k - \mu^{k-1}, (\mu_*^k - \mu^k) - (\mu_*^{k-1} - \mu^{k-1}) \rangle}{\langle \mu^k - \mu^{k-1}, \mu^k - \mu^{k-1} \rangle},$$

which approximately solves (in a least-squares sense) the following equation

$$\tau^k(\mu^k - \mu^{k-1}) \approx (\mu_*^k - \mu^k) - (\mu_*^{k-1} - \mu^{k-1}).$$

4 Numerical experiments and discussions

In order to illustrate the feasibility and efficiency of the proposed method, in this part, we present numerical experiments with electrical impedance tomography (EIT) of recovering the conductivity distribution from voltage measurements on the boundary based on sparsity constraints. EIT is one typical parameter identification problem for partial differential equations, and sparsity is a recent promising imaging technique [29, 27]. The reconstructions are obtained from experimental data with a water tank, immersed with plastic/metallic bars.

4.1 Mathematical model: Electrical impedance tomography

Electrical Impedance Tomography (EIT) is a non-destructive, low-cost and portable imaging modality developed for reconstructing the conductivity distribution in the interior of a concerned object. One typical experimental setup is as follows. One first attaches a set of metallic electrodes to the surface of the object, and then injects electrical currents into the object through these electrodes. The resulting potentials are then measured on the same set of electrodes. The inverse problem is then to infer the electrical conductivity distribution from these noisy measurements. It has found applications in many areas, including medical imaging and nondestructive evaluation.

The most accurate model for an EIT experiment, the complete electrode model (CEM), reads

$$\begin{cases} -\nabla \cdot (\sigma \nabla v) = 0 & \text{in } \Omega, \\ u + z_l \sigma \frac{\partial v}{\partial n} = V_l & \text{on } e_l, l = 1, \dots, L, \\ \int_{e_l} \sigma \frac{\partial v}{\partial n} ds = I_l & \text{for } l = 1, \dots, L, \\ \sigma \frac{\partial v}{\partial n} = 0 & \text{on } \Gamma \setminus \cup_{l=1}^L e_l, \end{cases} \quad (8)$$

where Ω denotes the domain occupied by the object and Γ is the boundary, σ is the electrical conductivity distribution, $v \in H^1(\Omega)$ is the electric potential, $\{e_l\}_{l=1}^L \subset \Gamma$ denote the surfaces under the L electrodes and n is the unit outward normal to the boundary Γ . In the model (8), z_l denotes contact impedance of the l th electrode caused by the resistive layer at the interface between the l th electrode and the object, and I_l and V_l are the electrode current and voltage, respectively, on the l th electrode. The currents $\{I_l\}_{l=1}^L$ satisfy the charge conservation law, and hence $\sum_{l=1}^L I_l = 0$. Upon introducing the subspace $\mathbb{R}_\Sigma^L = \{w \in \mathbb{R}^L : \sum_{l=1}^L w_l = 0\}$, we have $I := (I_1, \dots, I_L) \in \mathbb{R}_\Sigma^L$. Meanwhile, to ensure uniqueness of the solution to the model (8), the ground potential has to be fixed; this can be achieved, e.g., by requiring $\sum_{l=1}^L V_l = 0$, i.e., $V := (V_1, \dots, V_L) \in \mathbb{R}_\Sigma^L$. The model was first introduced in [10], and mathematically studied in [45, 28, 19]. In particular, for every strictly positive conductivity $\sigma \in L^\infty(\Omega)$ and current pattern $I \in \mathbb{R}_\Sigma^L$ and positive contact impedances $\{z_l\}_{l=1}^L$, there exists a unique solution $(v, V) \in H^1(\Omega) \times \mathbb{R}_\Sigma^L$ [45]. For a fixed current pattern I , we denote by $F(\sigma) = V(\sigma)$ the forward operator, and in the case of multiple input currents, we define $F(\sigma)$ by stacking respective potentials vectors. In the computation, we discard the potentials measured on current-carrying electrodes, which makes the model more robust with respect to contact impedances $\{z_l\}$. The inverse problem consists of inferring the physical conductivity σ^\dagger from the measured, thus noisy, electrode voltages V^δ .

There are many deterministic imaging algorithms for the EIT inverse problem. The Bayesian approach has gained increasing popularity in the last few years. The first substantial Bayesian modeling in EIT imaging was presented by Nicholls and Fox [40] and Kaipio et al [33]. In particular, in [33], Kaipio et al applied the Bayesian approach to EIT imaging, and systematically discussed various computational issues. West et al [51] studied the Bayesian formulation in medical applications of EIT, with an emphasis on incorporating explicit geometric information, e.g., anatomical structure and temporal correlation. The proper account of discretization errors and modeling errors has also received much recent attention; see e.g., [1, 41]. We refer to [50] for an overview of the status of statistical modeling in EIT imaging.

In this work, we adopt an approach based on sparsity constraints, which have demonstrated significant potentials in EIT imaging [27] and other parameter identification problems [29]. Now we build the probabilistic model as follows. First, we specify the likelihood function $p(V^\delta|\sigma)$. To this end, we assume

that the noisy voltages are contaminated by additive noises, i.e., $V^\delta = V(\sigma^\dagger) + \zeta$ for some noise vector ζ , and further, the noise components follow an independent and identically distributed Gaussian distribution with zero mean and inverse variance α . Then the likelihood function $p(V^\delta|\sigma)$ reads

$$p(V^\delta|\sigma) \propto e^{-\frac{\alpha}{2}\|F(\sigma)-V^\delta\|_2^2}$$

The prior distribution $p(\sigma)$ encodes our a priori knowledge or physical constraints on the sought-for conductivity distribution σ . First of all, the conductivity is pointwise non-negative due to physical constraints. Mathematically, the forward model (8) is not well defined for non-positive conductivities, and it degenerates if the conductivity tends to zero. Thus we enforce strict positivity on the conductivity σ using the characteristic function $\chi_{[\Lambda, \infty]}(\sigma_i)$ on each component with a small positive constant Λ . Second, we assume that the conductivity consists of a known (but possibly inhomogeneous) background $\sigma^{\text{bg}} \in \mathbb{R}^n$ plus some small inclusions. As is now widely accepted, one can encapsulate this ‘‘sparsity’’ assumption probabilistically by using a Laplace prior on the difference $\sigma - \sigma^{\text{bg}}$ of the sought-for conductivity σ from the background σ^{bg} :

$$\frac{\lambda}{2} e^{-\lambda\|\sigma - \sigma^{\text{bg}}\|_{\ell^1}},$$

where $\lambda > 0$ is a scale parameter, playing the same role of a regularization parameter in regularization methods. Intuitively, the ℓ_1 norm penalizes many small deviations from σ^{bg} stronger than a few big deviations, thereby favoring small and localized inclusions. We note that one may incorporate an additional smooth prior to enhance the cluster structure of typical inclusions

The Bayesian formulation involves two hyperparameters (α, λ) , and their choice is important for the reconstruction resolution. The inverse variance α should be available from the specification of the measurement equipment. The choice of the scale parameter λ (in the Laplace distribution) is much more involved. This is not surprising since it plays a role analogous to the regularization parameter in Tikhonov regularization, which is known to be highly nontrivial. One systematic way is to use hierarchical models [49], i.e., viewing the parameters as unknown random variables with their own (hyper-)priors. However, in general, an automated choice of the hyperparameters is still an actively researched topic. Here we have opted for an ad hoc approach: an initial value for λ was first estimated using a collection of typical reconstructions and then fine tuned by trial and error.

By Bayes’ formula, this leads to the following posterior distribution $p(\sigma|V^\delta)$ of the sought-for conductivity distribution σ

$$p(\sigma|V^\delta) \sim e^{-\frac{\alpha}{2}\|F(\sigma)-V^\delta\|_2^2} e^{-\lambda\|\sigma - \sigma^{\text{bg}}\|_{\ell^1}} \prod_{i=1}^n \chi_{[\Lambda, \infty]}(\sigma_i).$$

To apply the EP algorithm to the posterior $p(\sigma|V^\delta)$, we factorize it into

$$t_0(\sigma) = e^{-\frac{\alpha}{2}\|F(\sigma)-V^\delta\|_2^2},$$

$$t_i(\sigma) = e^{-\lambda|\sigma_i-\sigma_i^{\text{bg}}|\chi_{[\Lambda,\infty]}(\sigma_i)}, \quad i = 1, \dots, n.$$

Then the factor t_0 is Gaussian (after linearization, see Algorithm 4), and the remaining factors t_1, \dots, t_n each depend only on one component of σ . This enables us to rewrite the necessary integrals, upon appealing to Theorem 3.1, into one-dimensional ones. They have to be carried out semi-analytically, though, because a purely numerical quadrature may fail to deliver the required accuracy due to the singular shape of the Laplace prior, which is plagued with possible cancelation and underflow.

Finally, we briefly comment on the computational complexity of the EP algorithm. It needs n evaluations of the forward operator F to compute the linearized model F' in the outer iteration. Each evaluation of F is dominated by solving a linear problem of size $n \times n$, and for each outer evaluation the stiffness matrix remains unchanged and one can employ Cholesky decomposition to reduce the computational efforts. Further, it can be carried out in parallel if desired. Each inner iteration (linear EP) involves n EP updates, which is dominated by one Cholesky up/down-date of K and one forward/backward substitution. The cost of performing the low dimensional integration is negligible compared with other pieces. With k outer iterations and l inner iterations for each outer iteration, this gives a total cost of

$$O(kn^3/3 + kln(n + n^2/2)).$$

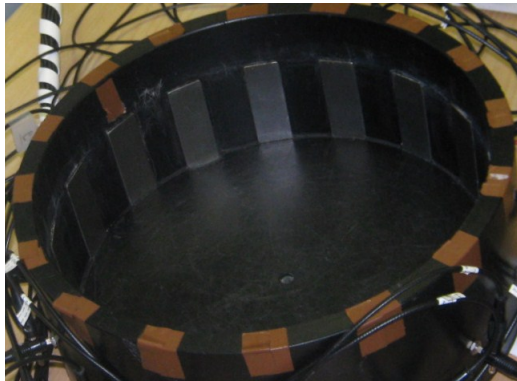
4.2 Numerical results and discussions

In this part, we illustrate the performance of the EP algorithm with real experimental data on a water tank. The measurement setup is illustrated in Fig. 1. The diameter of the cylindrical tank was 28 cm and the height was 10 cm. For the EIT measurements, sixteen equally spaced metallic electrodes (width 2.5 cm, height 7 cm) were attached to the inner surface of the tank. The tank was filled with tap water, and objects of different shapes and materials (either steel or plastic) were placed in the tank. We consider six cases listed in Table 1. All the inclusions were symmetric in height. In all cases, the excess water was removed from the tank, so that the height of water level was also 7 cm, the same as the height of the electrodes. The EIT measurements were conducted with the KIT 2 measurement system [43]. In these experiments, fifteen different current injections were carried out, between all adjacent electrode pairs. For each injection, 1 mA of current was injected into one electrode and the other electrode was grounded. Then the potentials of all other fifteen electrodes with respect to the grounded electrode were measured.

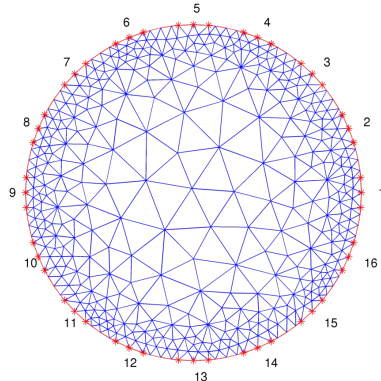
Due to cylindrical symmetry of the inclusions and the water tank, a two-dimensional CEM model was

Table 1: Description of experiments.

case	description
1	one plastic cylinder
2	two plastic cylinders
3	two neighboring plastic cylinders
4	three neighboring plastic cylinders
5	one plastic and one metallic cylinders
6	two plastic and one metallic cylinders



experimental setup



finite element mesh

Figure 1: The experimental setup and the finite element mesh for forward problems.

adequate for describing the solution of the EIT forward problem. We note that with the two-dimensional approximation of a cylindrical target, the conductivity σ represents the product γh , where γ is the (cylindrically symmetric) three-dimensional conductivity distribution and h is the height of the cylinder. Accordingly, z_l represents $z_l = \xi_l/h$, where ξ_l is the contact impedance in a three-dimensional model. The model was discretized by the piecewise linear finite element method, since the forward solution $u(\sigma)$ has only limited regularity, especially in the regions close to surface electrodes. The domain Ω was triangulated into a mesh with 424 nodes and 750 triangle elements, and the mesh is locally refined around the surface electrodes; see Fig. 1 for a schematic illustration. The conductivity is only computed on 328 inner nodes since it is fixed on the boundary. This is reasonable when the inclusions are in the interior, which is the case for our experiments. Further, the same finite element space was used for discretizing both the potential $u(\sigma)$ and the conductivity σ .

The contact impedances $\{z_l\}_{l=1}^L$ and the background conductivity σ^{bg} were determined from a separate experiment. That is, we carried out additional EIT measurements using tank filled solely with tap water. The estimation of the contact impedances $\{z_l\}_{l=1}^L$ and the constant background conductivity σ^{bg} is a well-posed problem; here, $\{z_l\}_{l=1}^L$ and σ^{bg} were reconstructed using the standard least-squares fitting [48]. The estimated background conductivity σ^{bg} was $1.41 \cdot 10^{-3} \Omega^{-1}$. In real (3D) conductivity units, this is $\gamma_{\text{bg}} = \sigma^{\text{bg}}/h = 1.41 \cdot 10^{-3} \Omega^{-1}/0.07 \text{ m} = 0.02 \Omega^{-1}\text{m}^{-1}$. This value is plausible – according to

literature, the conductivity of drinking water varies between $0.0005 \Omega^{-1}\text{m}^{-1}$ and $0.05 \Omega^{-1}\text{m}^{-1}$. The estimated contact impedances $\{z_l\}_{l=1}^L$ are shown in Table 2. Conversion to contact impedances in real units is obtained by multiplying the listed values by $h = 0.07 \text{ m}$.

Table 2: Estimated contact impedances $\{z_l\}$.

Electrode	1	2	3	4	5	6	7	8	9	10	11	12	13	14	15	16
$z_l(10^{-4}\Omega\text{m})$	2.64	3.00	2.76	4.27	3.50	4.30	3.91	2.35	2.01	2.21	2.04	1.43	2.98	2.78	2.92	3.40

The nonlinear EP algorithm was initialized with the estimated background conductivity σ^{bg} of tap water, and the Barzilai-Borwein stepsize τ_k was backtracked as $\tau_k = \max(0, \min(\tau_k, 1))$. The parameters of the distributions were set to $\alpha = 6.9 \times 10^4$ and $\lambda = 3.0 \times 10^4$ for all cases. To illustrate the accuracy of the EP algorithm, we present also the results by a standard Metropolis-Hastings MCMC algorithm (see Algorithm 1 for the complete procedure) with a normal random walker proposal distribution [35], with a sample size of 1.0×10^8 . The random walk stepsize is chosen such that the acceptance ratio is close to 0.234, which is known to be optimal [20]. It is well known that the convergence of MCMC methods is nontrivial to assess. Hence, we run eight chains in parallel with random and overdispersed initial values and different random seeds, and then compute the accuracy from these parallel chains. This enables us to directly compare the results of all chains by computing the maximum relative error of each chain from the mean of all chains. We also compute the Brooks-Gelman statistic [7], which compares the within-chain variance to the between-chain variance, and the statistics tends to one for convergent chains. In Table 3, we present the relative errors of the mean and the standard deviation, and the Brooks-Gelman statistics. It is observe that the chains for all cases, except case 1, converge reasonably well. In the first case, we could not obtain convergence, and hence the MCMC results for case 1 should be interpreted with care. In Fig. 2, we show the results of the eight MCMC chains for case 1. The means of the means and standard deviations for all eight chains are shown in blue, where the error bar is drawn as 1.96 times the standard deviation componentwise, which corresponds to the 95% credible interval for a one-dimensional Gaussian distribution. The componentwise minimum/maximum of expectation and standard deviation are drawn in red. The means agree well with each other, which further confirms the convergence of the chains. However, the accuracy of the standard deviation is not very high, even with the large number of MCMC samples.

Table 3: The accuracy of eight MCMC chains: relative errors in the mean and standard deviation, and Brooks-Gelman statistic.

case	1	2	3	4	5	6
mean	1.68e+0	8.60e-2	2.86e-2	7.03e-2	1.89e-2	8.78e-2
standard deviation	9.72e-1	7.72e-2	7.30e-2	1.53e-1	7.35e-2	1.51e-1
Brooks-Gelman	561.17	1.0069	1.0031	1.0045	1.0034	1.0139

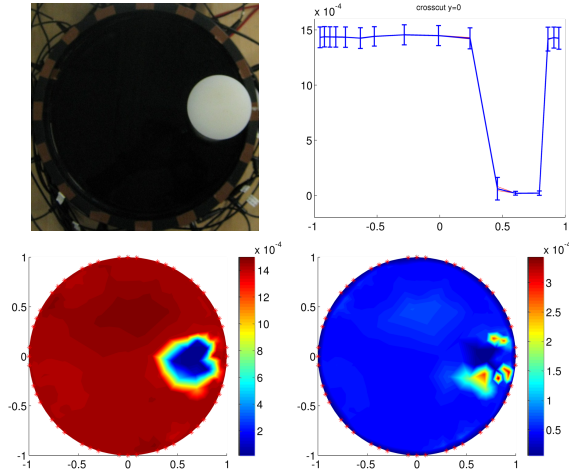


Figure 2: MCMC accuracy for case 1, one plastic inclusion. Top: Photography and horizontal cross-section with componentwise 95% intervals. Bottom: The mean of expectation and standard deviation of all eight chains.

The reconstructions using the serial EP algorithm took about 2 minutes with up to 7 outer iterations and a total of 22 inner iterations on a 2.6 GHz CPU, the MCMC algorithm took more than one day on a 2.4 GHz CPU. To show the convergence of the algorithm, in Fig. 3 we show the mean of the approximation \tilde{p} at intermediate iterates, where each row refers to one outer iteration. Further, in Table 4 we show the changes of the mean and covariance in the complete EP algorithm, i.e., Algorithm 4. In the table, we present the 2-norm of the difference at each iteration relative to the previous iterate and the last iterate (the converged approximation), which are indicated as $e_p(\mu)$ and $e_p(C)$ for the error relative to the previous iterate (respectively $e_f(\mu)$ and $e_f(C)$ for that relative to the last iterate). It is observed from the table that the errors decrease steadily as the EP iteration proceeds, and, like the MCMC algorithm, the convergence of the covariance is slower than that of the mean.

The results are shown in Figs. 4-9. In the figures, the left column shows a photography of the experiment, i.e., the watertank with the inclusions. The middle and right columns present the reconstructions by the EP algorithm and the MCMC method, respectively; the first and second rows present the posterior mean and the diagonal of the posterior standard deviation, respectively.

In all the experiments, EP and MCMC usually show a very good (mostly indistinguishable) match on the mean. For the variance, EP usually captures the same structure as MCMC, but the magnitudes are slightly different. The variance generally gets higher towards the center of the watertank (due to less information encapsulated in the measurements), and at the edges of detected inclusions (due to uncertainty in the edge's exact position). Further, compared with cases 1-4, the standard deviation of cases 5-6, which contains metallic bars, is much larger, i.e., the associated uncertainties are larger.

Finally, we observe that the Bayesian reconstructions with the Laplace prior contain many close-to-

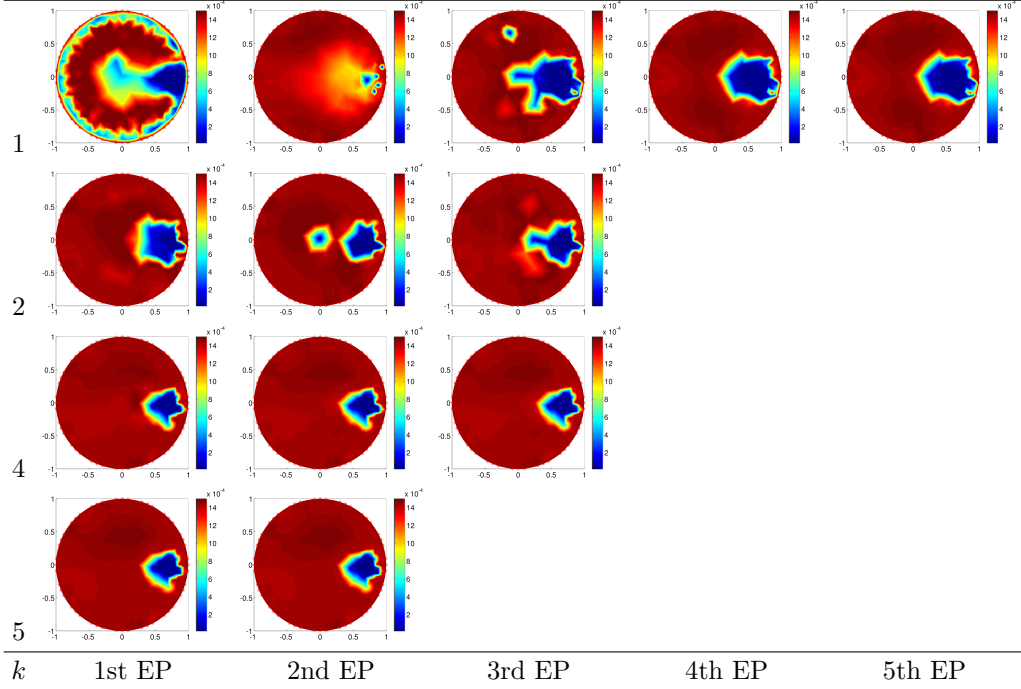


Figure 3: An illustration of the EP iterates for case 1. Plotted are the mean of each inner EP iterate, and each row refers to one outer iteration (k is the k th outer iteration).

zero components, however it is not truly sparse but only approximately sparse. This is different from the Tikhonov formulation, which yields a genuinely sparse reconstruction, as long as the regularization parameter is large enough; see the reconstructions in [19]. While the Tikhonov formulation yields only a point estimate, the EP reconstruction gives information about the mean, thus a weighted superposition of all possible reconstructions. The visually appealing sparsity of a Tikhonov minimizer can be misleading, because it only shows one solution in an ensemble of very different but (almost) equally probable reconstructions.

5 Conclusions

We presented a variational method for approximating the posterior probability distribution based on expectation propagation. The algorithm is of iterative nature, with each iteration matching the mean and covariances, by minimizing the Kullback-Leibler divergence. Some basic properties (convergence and stability) of the algorithm have been discussed. The algorithm is explicitly illustrated on a special class of posterior distributions which are of projection type. Numerically, we demonstrated the applicability to electrical impedance tomography with the complete electrode model on real experiments with a water tank immersed with plastic/metallic bars, under sparsity constraints. The numerical experiments indi-

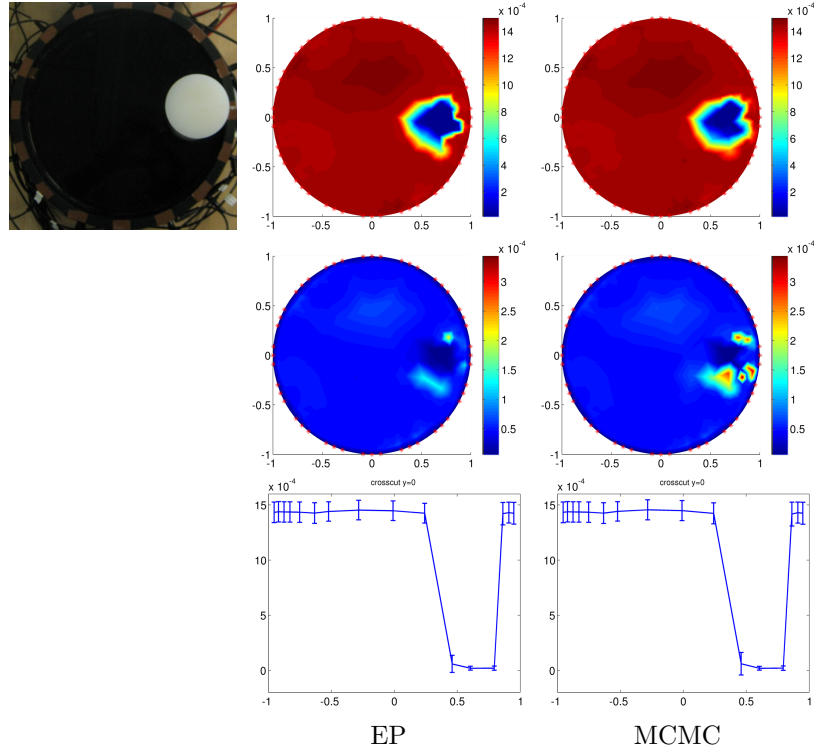


Figure 4: Numerical results for case 1, one plastic inclusion.

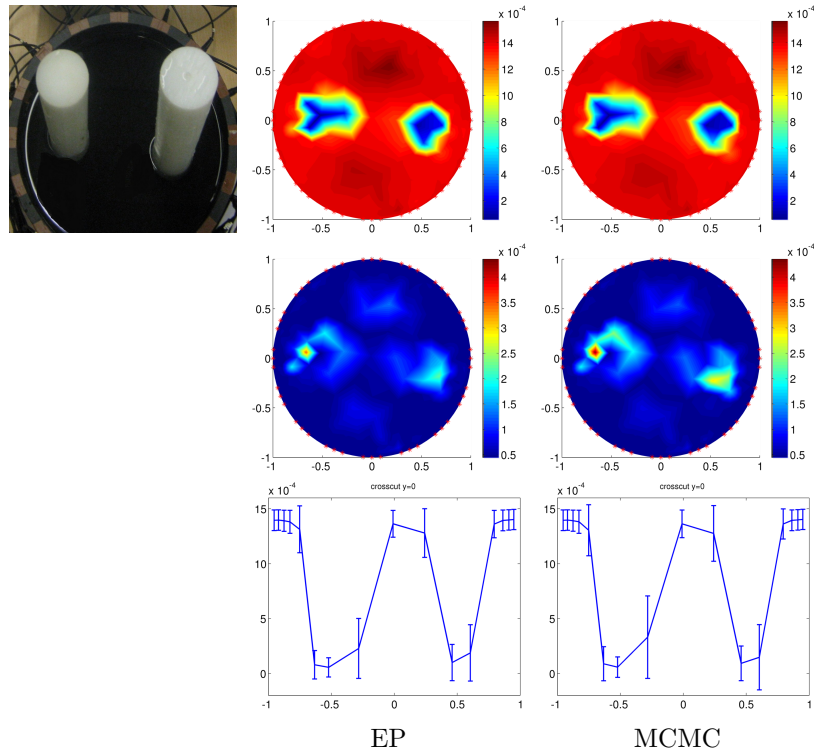


Figure 5: Numerical results for case 2, two plastic bars.

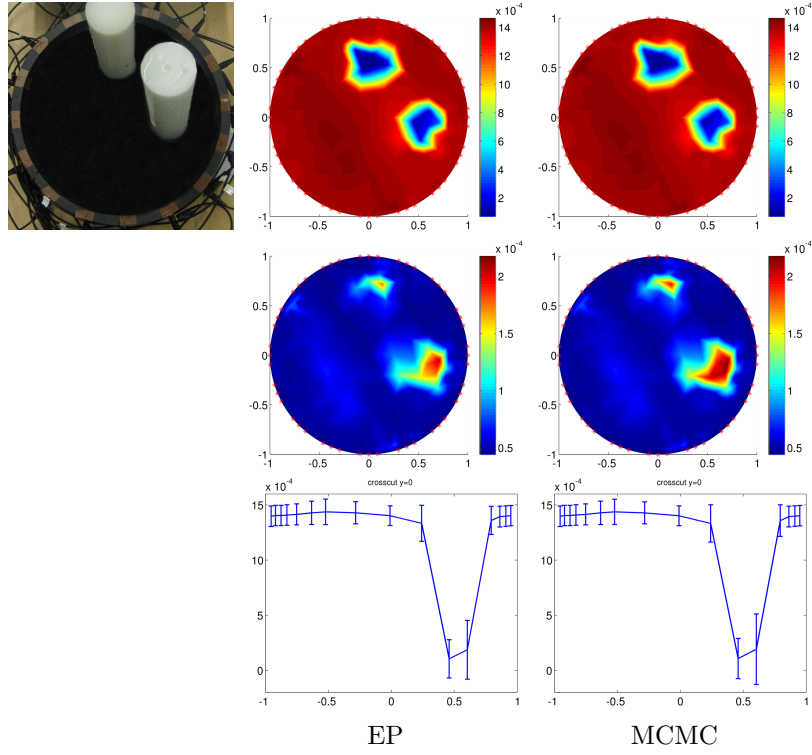


Figure 6: Numerical results for case 3, two neighboring plastic bars.

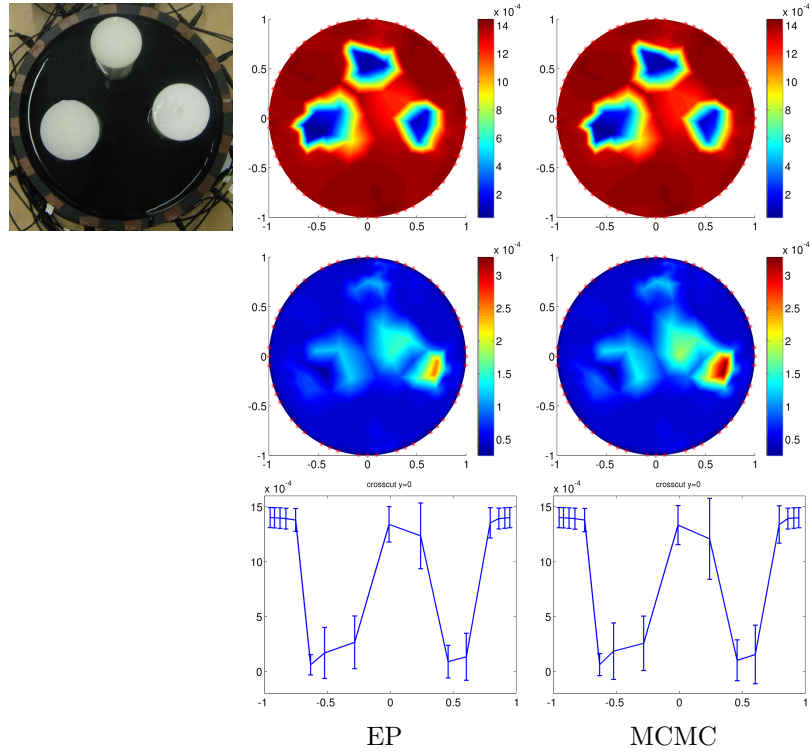


Figure 7: Numerical results for case 4, three neighboring plastic inclusions.

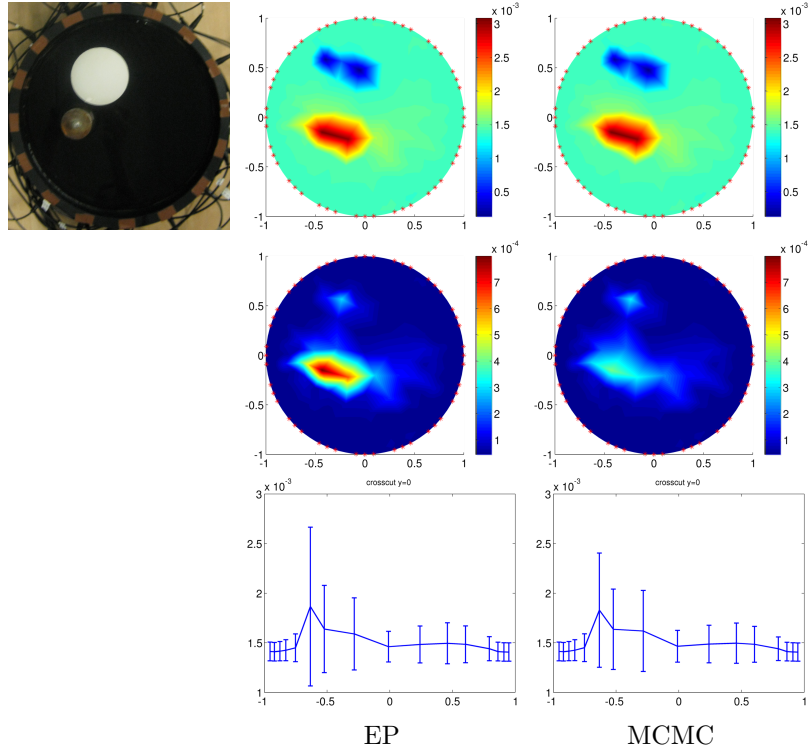


Figure 8: Numerical results for case 5, one plastic inclusion and one metallic inclusion.

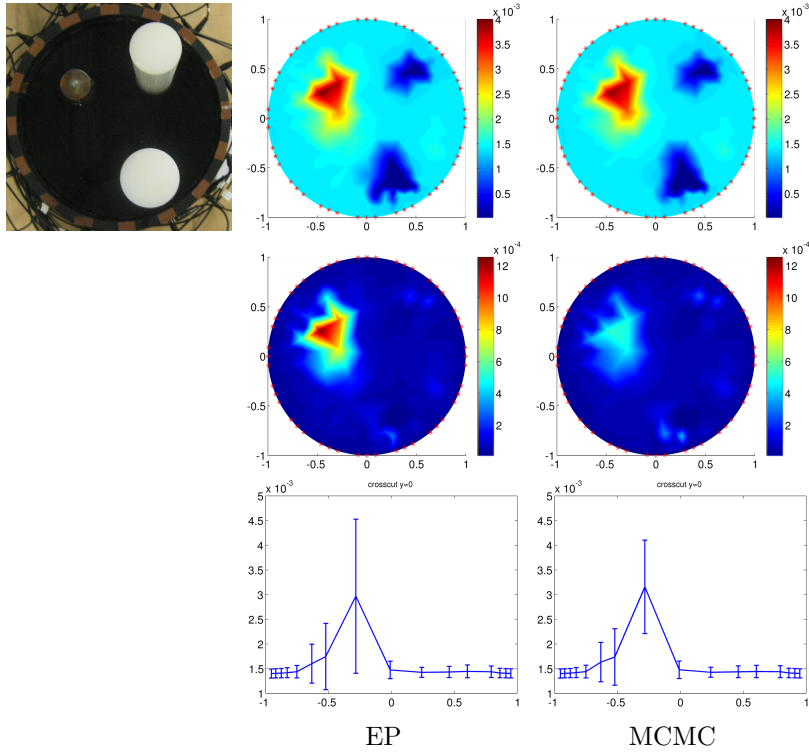


Figure 9: Numerical results for case 6, two plastic inclusions and one metallic inclusion.

Table 4: Convergence behavior of the EP algorithm for case 1. Here k and j refer respectively to the outer and inner iteration index, $e_p(\mu)$ and $e_p(C)$ denote the error relative of the mean μ and covariance C relative to the previous iterate, and $e_f(\mu)$ and $e_f(C)$ relative to the last iterate.

k	j	$e_p(\mu)$	$e_f(\mu)$	$e_p(C)$	$e_f(C)$
1	1	6.95e-1	6.21e-1	1.87e1	1.87e1
	2	7.23e-1	4.74e-1	1.87e1	1.82e0
	3	5.29e-1	2.53e-1	6.40e0	6.36e0
	4	1.71e-1	1.78e-1	5.57e0	3.69e0
	5	1.98e-3	1.78e-1	6.76e-1	3.54e0
2	1	2.40e-1	2.26e-1	1.15e0	4.03e0
	2	2.58e-1	1.71e-1	3.96e0	2.55e0
	3	1.60e-1	1.04e-1	2.60e0	3.07e0
	4	2.86e-2	9.63e-2	2.54e0	3.56e0
	5	1.58e-3	9.63e-2	2.75e-1	3.67e0
3	1	1.46e-1	1.21e-1	1.23e0	3.85e0
	2	1.07e-1	5.74e-2	3.54e0	8.67e-1
	3	4.45e-2	3.39e-2	6.83e-1	7.92e-1
	4	2.32e-2	4.47e-2	4.48e-1	4.62e-1
	5	4.39e-3	4.34e-2	3.06e-1	7.06e-1
4	1	3.11e-2	2.36e-2	1.04e-1	6.97e-1
	2	1.11e-2	1.74e-2	4.56e-1	2.90e-1
	3	1.91e-3	1.79e-2	2.17e-1	3.35e-1
5	1	1.80e-2	1.28e-3	1.94e-1	1.58e-1
	2	1.28e-3	0.00e0	1.58e-1	0.00e0

cate that compared with Markov chain Monte Carlo methods, the expectation propagation algorithm is computationally very efficient, and reasonably accurate.

Even though we showcase only the electrical impedance tomography, expectation propagation clearly can be applied to a wide variety of other nonlinear inverse problems, e.g., optical tomography and inverse scattering. In addition, there are several avenues for further research. First, it is important to extend the algorithm to other important prior distributions (e.g., total variation and nonlog-concave sparsity-promoting priors) and likelihood functions (e.g., Laplace/ t distributions for robust formulations). We note that these extensions are nontrivial for parameter identifications. For example, for the total variation prior, one complicating factor is the presence of box constraints, whose treatment is not straightforward; whereas the absence of log concavity poses severe numerical stability issues. Second, we have described some basic properties of the EP algorithm. However, many fundamental properties, e.g., its global and local convergence properties, and stability with respect to data perturbation, remains elusive. Third, the computational efficiency of the EP algorithm requires careful implementation, e.g., computing the diagonal elements of the inverse of large (and possibly dense) inverse covariance matrix and accurate

numerical quadrature of low-dimensional but nonsmooth integrals. This necessitates the study of relevant numerical issues, e.g., semi-analytic formulas and error estimates.

Acknowledgements

The authors would like to thank the referees for their helpful comments, and thank Dr. Aku Seppänen of University of Eastern Finland for kindly providing the experimental data. The work was initiated during MG’s visit at Texas A&M University, supported partially by a scholarship by Deutscher Akademischer Austausch Dienst (DAAD) and a visitor programme of Institute for Applied Mathematics and Computational Science, Texas A&M University. The work of BJ was partially supported by NSF Grant DMS-1319052.

A Proof of Proposition 2.2

Proof. We recast the posterior $p(x)$ into the formulation (3) for EP with projection

$$p(x) = \prod t_i(U_i x),$$

where the matrices U_i consist of disjoint rows of the identity matrix $I_n \in \mathbb{R}^{n \times n}$. Upon relabeling the variables, we may assume $[U_1^t \dots U_k^t] = I_n$. Then the Gaussian approximations $\{\tilde{t}_i\}$ take the form

$$\tilde{t}_i(x) = G(x, U_i^t h_i, U_i^t K_i U_i) \sim e^{-\frac{1}{2} x^t U_i^t K_i U_i x + h_i^t U_i x},$$

where $K_i \in \mathbb{R}^{r \times r}$ and $h_i \in \mathbb{R}^r$, with r being the cardinality of x_i . The Gaussian approximation $\tilde{p}(x) = G(x, h, K)$ to $p(x)$ is given by the product of factor approximations, i.e., $h = \sum_i U_i^t h_i$ and $K = \sum_i U_i^t K_i U_i$. By the construction of U_i , the matrix K is block diagonal with blocks K_i . Further, to update the i -th factor, steps 6 and 8 of Algorithm 3 yield $\widehat{C}_i^{-1} = (U_i K^{-1} U_i^t)^{-1} - K_i = 0$ and hence

$$K_i = \text{Var}_{Z^{-1}t_i(s_i)N(s_i; \widehat{\mu}_i, \widehat{C}_i)}[s_i]^{-1} - \widehat{C}_i^{-1} = \text{Var}_{Z^{-1}t_i(s_i)}[s_i]^{-1}.$$

Thus the update K_i depends only on t_i , but not on the current approximation, from which the one-sweep convergence follows directly. \square

B Auxiliary lemmas

Below, we recall some results on exponential family [8]. We shall only need their specialization to normal distributions, but we follow the general framework for two reasons: it is the usual form found in the literature, and it allows direct generalization from normal distributions to other exponential families.

Definition B.1. *An exponential family is a set \mathcal{F} of distributions with density of the form*

$$p(x|\theta) = e^{\theta^t \phi(x) - \Phi(\theta)},$$

$$\Phi(\theta) = \log \int e^{\theta^t \phi(x)} d\nu(x),$$

for natural parameter θ from the natural parameter space Θ . The exponential family is fully characterized by the sufficient statistics ϕ and the base measure $d\nu$. The natural parameter space Θ is a convex set of all natural parameters such that $p(x|\theta)$ is a valid distribution.

The log partition function Φ allows computing the mean and variance of $\phi(x)$:

$$\nabla_{\theta} \Phi = E_{p(x|\theta)}[\phi(x)] \quad \text{and} \quad \nabla_{\theta}^2 \Phi = \text{Var}_{p(x|\theta)}[\phi(x)]. \quad (9)$$

Let $f(x)$ be a positive function, and $\log E_{p(x|\theta)}[f(x)] + \Phi(\theta)$ exists for every $\theta \in \Theta$. Then it defines a new exponential family with the base measure $f(x)d\nu(x)$, with the log partition function $\Phi_f(\theta)$ given by $\log E_{p(x|\theta)}[f(x)] + \Phi(\theta)$.

We now consider the exponential family of normal distributions. We denote a normal distribution with mean μ and covariance C by $N(x; \mu, C) = (2\pi)^{-\frac{n}{2}} (\det C)^{-\frac{1}{2}} e^{-\frac{1}{2}(x-\mu)^t C^{-1}(x-\mu)}$. Hence, the sufficient statistics $\phi(x)$ and the natural parameter θ are given by $\phi(x) = (x, xx^t)$, and $\theta =: (h, K) = (C^{-1}\mu, -\frac{1}{2}C^{-1})$, respectively. This together with (9) and the chain rule yields

$$E_{N(x;\mu,C)}[x] = C \nabla_{\mu} \Phi(\theta(\mu, C)) \quad \text{and} \quad \text{Var}_{N(x;\mu,C)}[x] = C \nabla_{\mu}^2 \Phi(\theta(\mu, C)) C.$$

Now we can state a result on a tilted normal distribution $f(x)N(x, \mu, C)$.

Lemma B.1. *Let $N(x; \mu, C)$ be a normal distribution and f a positive function. Then the mean μ_f and covariance C_f of the tilted distribution $Z^{-1}f(x)N(x; \mu, C)$ ($Z = \int f(x)N(x; \mu, C)$) are given by*

$$\mu_f = C (\nabla_{\mu} \log E_{N(x;\mu,C)}[f(x)]) + \mu,$$

$$C_f = C (\nabla_{\mu}^2 \log E_{N(x;\mu,C)}[f(x)]) C + C.$$

Proof. Let Φ and Φ_f be the log partition function of the normal distribution $p(x|\theta) = N(x; \mu, C)$ and the

tilted distribution $\tilde{p}(x|\theta) = f(x)N(x; \mu, C)e^{-\Phi_f}$, respectively, with $\theta(\mu, C) = (h, K) = (C^{-1}\mu, -\frac{1}{2}C^{-1})$. Then $\Phi_f(\theta) = \log E_{p(x|\theta)}[f(x)] + \Phi(\theta)$. Further, the first component of (9) reads

$$\nabla_h \Phi_f(\theta) = E_{\tilde{p}(x|\theta)}[x] \quad \text{and} \quad \nabla_h^2 \Phi_f(\theta) = \text{Var}_{\tilde{p}(x|\theta)}[x].$$

By the chain rule there hold

$$\begin{aligned} \nabla_\mu \log E_{N(x;\mu,C)}[f(x)] &= C^{-1} \nabla_h \log E_{p(x|\theta)}[f(x)], \\ \nabla_\mu^2 \log E_{N(x;\mu,C)}[f(x)] &= C^{-1} \nabla_h^2 \log E_{p(x|\theta)}[f(x)] C^{-1}. \end{aligned}$$

Consequently, we deduce

$$\begin{aligned} E_{\tilde{p}(x|\theta)}[x] &= \nabla_h \Phi_f(\theta) = C \nabla_\mu \log E_{N(x;\mu,C)}[f(x)] + \nabla_h \Phi(\theta), \\ \text{Var}_{\tilde{p}(x|\theta)}[x] &= \nabla_h^2 \Phi_f(\theta) = C \nabla_\mu^2 \log E_{N(x;\mu,C)}[f(x)] C + \nabla_h^2 \Phi(\theta). \end{aligned}$$

Now the desired assertion follows directly from the relation $\nabla_h \Phi(\theta) = \mu$ and $\nabla_h^2 \Phi(\theta) = C$ using (9). \square

Lemma B.2. *Let $p : \mathbb{R}^n \rightarrow \mathbb{R}$ be a probability density function with a support of positive measure. If the covariance $\text{Var}_p[x] = \int p(x)(E[x] - x)(E[x] - x)^t dx$ exists, then it is positive definite.*

Proof. It suffices to show $w^t \text{Var}_p[x] w > 0$ for any nonzero vector $w \in \mathbb{R}^n$. Let $S = \{x \in \text{supp}(p) : w^t(E[x] - x) \neq 0\}$. However, the complement set $\text{supp}(p) \setminus S = \{x \in \text{supp}(p) : w^t(E[x] - x) = 0\}$ lies in a co-dimensional one hyperplane in \mathbb{R}^n , thus it has only zero measure. This together with the positive measure assumption of the support $\text{supp}(p)$, the set S has positive measure. Therefore, $w^t \text{Var}_p[x] w \geq \int_S p(x)(w^t(E[x] - x))^2 dx > 0$. \square

Finally we recall the concept of log-concavity. It plays a role in the theory of expectation propagation as convexity in classical optimization theory. A nonnegative function $f : V \rightarrow \mathbb{R}_0^+$ is log-concave if

$$f(\lambda x_1 + (1 - \lambda)x_2) \geq f(x_1)^\lambda f(x_2)^{1-\lambda}$$

holds for all elements x_1, x_2 from a real convex vector space V and for all $\lambda \in [0, 1]$.

Lemma B.3. *Let $f, g : V \rightarrow \mathbb{R}_0^+$ be log-concave. Then the product fg is log-concave.*

Log-concavity is preserved by marginalization by the Prékopa-Leindler inequality [5, Corollary 1.8.3] [6, Corollary 3.5].

Lemma B.4. *Let $f : \mathbb{R}^n \times \mathbb{R}^m \rightarrow \mathbb{R}_0^+$ be log-concave and bounded. Then the marginalized function $g(x) = \int f(x, y) dy$ is log-concave.*

C Proof of Theorem 3.1

We begin with an elementary lemma, which shows that the normalizing constant of the product density is invariant under linear transformation.

Lemma C.1. *Let $x \sim N(x; \mu, C)$ with $C \in \mathbb{R}^{n \times n}$ being symmetric positive definite and $U \in \mathbb{R}^{l \times n}$ ($l \leq n$) be of full row rank. Then*

$$\int t(Ux)N(x; \mu, C) dx = \int t(s)N(s; U\mu, UCU^t) ds.$$

Proof. Let $T \in \mathbb{R}^{n \times n}$ be a bijective completion of U , i.e., there is some $R \in \mathbb{R}^{(n-l) \times n}$, such that $T = \begin{bmatrix} U \\ R \end{bmatrix}$.

Further, we denote $Tx = \begin{pmatrix} s = Ux \\ r = Rx \end{pmatrix} := \hat{x}$. Then we have

$$\frac{1}{(2\pi)^{\frac{n}{2}} \sqrt{\det C}} e^{-\frac{1}{2}(\mu-x)^t C^{-1}(\mu-x)} = \frac{1}{(2\pi)^{\frac{n}{2}} \sqrt{\det C}} e^{-\frac{1}{2}(T\mu-Tx)^t (TCT^t)^{-1}(T\mu-Tx)} = |\det T| N(Tx; T\mu, TCT^t).$$

Consequently,

$$\int t(Ux)N(x, \mu, C) dx = \int t(Ux) |\det T| N(Tx; T\mu, TCT^t) dx = \int t(s)N(\hat{x}; T\mu, TCT^t) d\hat{x}.$$

Now we split the Gaussian distribution $N(\hat{x}; T\mu, TCT^t)$ into

$$N(\hat{x}; T\mu, TCT^t) = N(s; U\mu, UCU^t)N(r; \hat{\mu}(s), \hat{C}), \quad (10)$$

where $\hat{\mu}(s) = R\mu + (UCR^t)^t(UCU^t)^{-1}(s - U\mu)$, and $\hat{C} = RCR^t - (UCR^t)^t(UCU^t)^{-1}(UCR^t)$ is the Schur complement of UCU^t . Therefore,

$$\begin{aligned} \int t(Ux)N(x; \mu, C) dx &= \int t(s)N(s; U\mu, UCU^t) \int N(r; \hat{\mu}(s), \hat{C}) dr ds \\ &= \int t(s)N(s; U\mu, UCU^t) ds. \end{aligned}$$

□

Now we present the proof of Theorem 3.1.

Proof. Let $Z = \int t(Ux)N(x; \mu, C)x dx$. By Lemma C.1, $Z = \int t(s)N(s; U\mu, UCU^t) ds$. Now using the

completion T of U and the splitting (10), we can write

$$\begin{aligned}
T \int Z^{-1}t(Ux)N(x; \mu, C)x \, dx &= \int Z^{-1}t(s)N(s; U\mu, UCU^t) \int N(r; \hat{\mu}(s), \hat{C})\hat{x} \, dr \, ds \\
&= \int Z^{-1}t(s)N(s; U\mu, UCU^t) \begin{pmatrix} s \\ \hat{\mu}(s) \end{pmatrix} \, ds \\
&= \begin{pmatrix} E_{Z^{-1}t(s)N(s; U\mu, UCU^t)}[s] \\ R\mu + (UCR^t)^t(UCU^t)^{-1}(E_{Z^{-1}t(s)N(s; U\mu, UCU^t)}[s] - U\mu) \end{pmatrix}.
\end{aligned}$$

The unique solution $\mu^* := E_{Z^{-1}t(Ux)N(x; \mu, C)}[x]$ of this matrix equation is given by

$$\mu^* = \mu + CU^t(UCU^t)^{-1}(\bar{s} - U\mu),$$

where $\bar{s} = E_{Z^{-1}t(s)N(s; U\mu, UCU^t)}[s]$. This shows the first identity.

We turn to the covariance $C^* = E_{Z^{-1}t(Ux)N(x; \mu, C)}[(x - \mu^*)(x - \mu^*)^t]$. With a change of variable and the splitting (with $\bar{s} = U\mu^*$ and $\bar{r} = R\mu^*$)

$$(\hat{x} - T\mu^*)(\hat{x} - T\mu^*)^t = \begin{pmatrix} (s - \bar{s})(s - \bar{s})^t & (s - \bar{s})(r - \bar{r})^t \\ (r - \bar{r})(s - \bar{s})^t & (r - \bar{r})(r - \bar{r})^t \end{pmatrix},$$

we deduce that

$$\begin{aligned}
TC^*T^t &= \int Z^{-1}t(s)N(s; U\mu, UCU^t) \int N(r; \hat{\mu}(s), \hat{C})(\hat{x} - T\mu^*)(\hat{x} - T\mu^*)^t \, dr \, ds \\
&= \int Z^{-1}t(s)N(s; U\mu, UCU^t) \begin{pmatrix} (s - \bar{s})(s - \bar{s})^t & (s - \bar{s})(\hat{\mu}(s) - \bar{r})^t \\ (\hat{\mu}(s) - \bar{r})(s - \bar{s})^t & \hat{C} + (\hat{\mu}(s) - \bar{r})(\hat{\mu}(s) - \bar{r})^t \end{pmatrix} \, ds.
\end{aligned}$$

Further, it follows from (10) that $\hat{\mu}(s) - \bar{r} = (UCR^t)^t(UCU^t)^{-1}(s - \bar{s}) := L(s - \bar{s})$. Consequently, the covariance C^* satisfies

$$\begin{pmatrix} UC^*U^t & UC^*R^t \\ RC^*U^t & RC^*R^t \end{pmatrix} = \begin{pmatrix} \bar{C} & \bar{C}L^t \\ L\bar{C} & L\bar{C}L^t + \hat{C} \end{pmatrix}$$

where $\bar{C} = E_{Z^{-1}t(s)N(s; U\mu, UCU^t)}[(s - \bar{s})(s - \bar{s})^t]$. The unique solution C^* to the equation is given by

$$C^* = C + CU^t(UCU^t)^{-1}(\bar{C} - UCU^t)(UCU^t)^{-1}UC,$$

which can be verified directly termwise. This shows the second identity. \square

References

- [1] S. R. Arridge, J. P. Kaipio, V. Kolehmainen, M. Schweiger, E. Somersalo, T. Tarvainen, and M. Vauhkonen. Approximation errors and model reduction with an application in optical diffusion tomography. *Inverse Problems*, 22(1):175–195, 2006.
- [2] J. Barzilai and J. M. Borwein. Two-point step size gradient methods. *IMA J. Numer. Anal.*, 8(1):141–148, 1988.
- [3] M. J. Beal. *Variational Algorithms for Approximate Bayesian Inference*. PhD thesis, Gatsby Computational Neuroscience Unit, University College London, 2003.
- [4] I. Billionis and N. Zabaras. A stochastic optimization approach to coarse-graining using a relative-entropy framework. *J. Chem. Phys.*, 138(4):044313, 12 pp., 2013.
- [5] V. I. Bogachev. *Gaussian Measures*, volume 62 of *Mathematical Surveys and Monographs*. American Mathematical Society, Providence, RI, 1998.
- [6] H. J. Brascamp and E. H. Lieb. On extensions of the Brunn-Minkowski and Prékopa-Leindler theorems, including inequalities for log concave functions, and with an application to the diffusion equation. *J. Fun. Anal.*, 22(4):366–389, 1976.
- [7] S. P. Brooks and A. Gelman. General methods for monitoring convergence of iterative simulations. *J. Comput. Graph. Statist.*, 7(4):434–455, 1998.
- [8] L. D. Brown. *Fundamentals of Statistical Exponential Families with Applications in Statistical Decision Theory*. Institute of Mathematical Statistics, Hayward, CA, 1986.
- [9] A. Chaimovich and M. S. Shell. Coarse-graining errors and numerical optimization using a relative entropy framework. *J. Chem. Phys.*, 134(9):094112, 15 pp., 2011.
- [10] K.-S. Cheng, D. Isaacson, J. C. Newell, and D. G. Gisser. Electrode models for electric current computed tomography. *IEEE Trans. Biomed. Eng.*, 36(9):918–924, 1989.
- [11] J. A. Christen and C. Fox. Markov chain Monte Carlo using an approximation. *J. Comput. Graph. Statist.*, 14(4):795–810, 2005.
- [12] C. Clason and B. Jin. A semi-smooth Newton method for nonlinear parameter identification problems with impulsive noise. *SIAM J. Imaging Sci.*, 5(2):505–538, 2012.

- [13] P. S. Dwyer. Some applications of matrix derivatives in multivariate analysis. *J. Amer. Stat. Assoc.*, 62(318):607–625, 1967.
- [14] Y. Efendiev, T. Hou, and W. Luo. Preconditioning Markov chain Monte Carlo simulations using coarse-scale models. *SIAM J. Sci. Comput.*, 28(2):776–803, 2006.
- [15] T. A. El Moselhy and Y. M. Marzouk. Bayesian inference with optimal maps. *J. Comput. Phys.*, 231(23):7815–7850, 2012.
- [16] H. P. Flath, L. C. Wilcox, V. Akçelik, J. Hill, B. van Bloemen Waanders, and O. Ghattas. Fast algorithms for Bayesian uncertainty quantification in large-scale linear inverse problems based on low-rank partial Hessian approximations. *SIAM J. Sci. Comput.*, 33(1):407–432, 2011.
- [17] J. N. Franklin. Well-posed stochastic extensions of ill-posed linear problems. *J. Math. Anal. Appl.*, 31(3):682–716, 1970.
- [18] J. Gao. Robust L1 principal component analysis and its Bayesian variational inference. *Neur. Comput.*, 20(2):555–572, 2008.
- [19] M. Gehre, T. Kluth, A. Lipponen, B. Jin, A. Seppänen, J. P. Kaipio, and P. Maass. Sparsity reconstruction in electrical impedance tomography: an experimental evaluation. *J. Comput. Appl. Math.*, 236(8):2126–2136, 2012.
- [20] A. Gelman, G. O. Roberts, and W. R. Gilks. Efficient Metropolis jumping rules. In J. M. Bernardo, J. O. Berger, A. P. Dawid, and A. F. M. Smith, editors, *Bayesian Statistics 5*, pages 599–607. Oxford University Press, 1996.
- [21] W. R. Gilks, S. Richardson, and D. J. Spiegelhalter. *Markov Chain Monte Carlo in Practice*. Chapman and Hall, London, 1996.
- [22] P. E. Gill, G. H. Golub, W. Murray, and M. A. Saunders. Methods for modifying matrix factorizations. *Math. Comput.*, 28(126):505–535, 1974.
- [23] M. Girolami and B. Calderhead. Riemann manifold Langevin and Hamiltonian Monte Carlo methods. *J. R. Stat. Soc. Ser. B Stat. Methodol.*, 73(2):123–214, 2011.
- [24] D. Higdon, H. Lee, and Z. Bi. A Bayesian approach to characterizing uncertainty in inverse problems using coarse and fine-scale information. *IEEE Trans. Sign. Proc.*, 50(2):389–399, 2002.
- [25] B. Jin. Fast Bayesian approach for parameter estimation. *Int. J. Numer. Methods Engrg.*, 76(2):230–252, 2008.

- [26] B. Jin. A variational Bayesian method to inverse problems with impulsive noise. *J. Comput. Phys.*, 231(2):423–435, 2012.
- [27] B. Jin, T. Khan, and P. Maass. A reconstruction algorithm for electrical impedance tomography based on sparsity regularization. *Int. J. Numer. Methods Engrg.*, 89(3):337–353, 2012.
- [28] B. Jin and P. Maass. An analysis of electrical impedance tomography with applications to tikhonov regularization. *ESAIM: Control. Optim. Cal. Var.*, 18(4):1027–1048, 2012.
- [29] B. Jin and P. Maass. Sparsity regularization for parameter identification problems. *Inverse Problems*, 28(12):123001, 70 pp., 2012.
- [30] M. I. Jordan, Z. Ghahramani, T. S. Jaakkola, and L. K. S. Saul. An introduction to variational methods for graphical models. *Mach. Learn.*, 37(2):183–233, 1999.
- [31] S. Kaczmarz. Angenäherte Auflösung von Systemen linearer Gleichungen. *Bull. Acad. Pol. Sci. Lett. A*, 35:355–357, 1937.
- [32] J. Kaipio and E. Somersalo. *Statistical and Computational Inverse Problems*. Springer-Verlag, New York, 2005.
- [33] J. P. Kaipio, V. Kolehmainen, E. Somersalo, and M. Vauhkonen. Statistical inversion and Monte Carlo sampling methods in electrical impedance tomography. *Inverse Problems*, 16(5):1487–1522, 2000.
- [34] S. Kullback and R. A. Leibler. On information and sufficiency. *Ann. Math. Statistics*, 22(1):79–86, 1951.
- [35] J. Liu. *Monte Carlo Strategies in Scientific Computing*. Springer, Berlin, 2008.
- [36] J. Martin, L. C. Wilcox, C. Burstedde, and O. Ghattas. A stochastic Newton MCMC method for large-scale statistical inverse problems with application to seismic inversion. *SIAM J. Sci. Comput.*, 34(3):A1460–A1487, 2012.
- [37] Y. M. Marzouk, H. N. Najm, and L. A. Rahn. Stochastic spectral methods for efficient Bayesian solution of inverse problems. *J. Comput. Phys.*, 224(2):560–586, 2007.
- [38] T. Minka. Expectation propagation for approximate Bayesian inference. In J. Breese and D. Koller, editors, *Uncertainty in Artificial Intelligence 17*. Morgan Kaufmann, 2001.
- [39] T. Minka. *A Family of Algorithms for Approximate Bayesian inference*. PhD thesis, Massachusetts Institute of Technology, 2001.

- [40] G. K. Nicholls and C. Fox. Prior modelling and posterior sampling in impedance imaging. *Proc. SPIE*, 3459:116–127, 1998.
- [41] A. Nissinen, L. M. Heikkinen, and J. P. Kaipio. The bayesian approximation error approach for electrical impedance tomography: experimental results. *Meas. Sci. Tech.*, 19(1):015501, 9pp, 2008.
- [42] M. Opper and O. Winther. Expectation consistent approximate inference. *J. Mach. Learn. Res.*, 6:2177–2204, 2005.
- [43] T. Savolainen, L. Heikkinen, M. Vauhkonen, and J. Kaipio. A modular, adaptive electrical impedance tomography system. In *Proc. 3rd World Congress on Industrial Process Tomography, Banff, Canada*, pages 50–55, 2003.
- [44] M. W. Seeger. Bayesian inference and optimal design for the sparse linear model. *J. Mach. Learn. Res.*, 9:759–813, 2008.
- [45] E. Somersalo, M. Cheney, and D. Isaacson. Existence and uniqueness for electrode models for electric current computed tomography. *SIAM J. Appl. Math.*, 52(4):1023–1040, 1992.
- [46] O. Stramer and R. L. Tweedie. Langevin-type models II: self-targeting candidates for MCMC algorithms. *Methodol. Comput. Appl. Prob.*, 1(3):307–328, 1999.
- [47] M. A. J. van Gerven, B. Cseke, F. P. de Lange, and T. Heskes. Efficient Bayesian multivariate fMRI analysis using a sparsifying spatio-temporal prior. *NeuroImage*, 50(1):150–161, 2010.
- [48] T. Vilhunen, J. P. Kaipio, P. J. Vauhkonen, T. Savolainen, and M. Vauhkonen. Simultaneous reconstruction of electrode contact impedances and internal electrical properties: I. Theory. *Meas. Sci. Tech.*, 13(12):1848–1854, 2002.
- [49] J. Wang and N. Zabaras. Hierarchical Bayesian models for inverse problems in heat conduction. *Inverse Problems*, 21(1):183–206, 2005.
- [50] D. Watzenig and C. Fox. A review of statistical modelling and inference for electrical capacitance tomography. *Meas. Sci. Tech.*, 20(5):052002, 22 pp., 2009.
- [51] R. West, R. Aykroyd, S. Meng, and R. Williams. Markov chain Monte Carlo techniques and spatial-temporal modelling for medical EIT. *Physiol. Meas.*, 25(1):181–194, 2004.
- [52] M. A. Woodbury. *Inverting modified matrices*. Statistical Research Group, Memo. Rep. no. 42. Princeton University, Princeton, N. J., 1950.